UNCLASSIFIED

AD NUMBER
AD875995

LIMITATION CHANGES

TO:

Approved for public release; distribution is unlimited.

FROM:

Distribution authorized to U.S. Gov't. agencies and their contractors; Critical Technology; OCT 1970. Other requests shall be referred to Air Force Arnold Engineering Development Center, Attn: XON, Arnold AFB, TN 37389. This document contains export-controlled technical data.

AUTHORITY

aedc, usaf ltr, 31 May 1972

THIS PAGE IS UNCLASSIFIED

AEDC-TR-70-218

DETERMINATION OF
TRANSITION REYNOLDS NUMBER IN THE
TRANSONIC MACH NUMBER RANGE

O. P. Credle and W. E. Carleton

ARO, Inc.

October 1970

PROPULSION WIND TUNNEL FACILITY
ARNOLD ENGINEERING DEVELOPMENT CENTER
AIR FORCE SYSTEMS COMMAND
ARNOLD AIR FORCE STATION, TENNESSEE

NOTICES

DETERMINATION OF
TRANSITION REYNOLDS NUMBER IN THE
TRANSONIC MACH NUMBER RANGE

O. P. Credle and W. E. Carleton

ARO, Inc.

FOREWORD

The work reported herein was sponsored by Arnold Engineering Development Center (AEDC), Air Force Systems Command (AFSC), under Program Element 65401F/G226.

The test results presented were obtained by ARO, Inc. (a subsidiary of Sverdrup & Parcel and Associates, Inc.), contract operator of AEDC, AFSC, Arnold Air Force Station, Tennessee, under Contract F40600-71-C-0002. The work was conducted under ARO Project No. PT2059 from December 1969 to June 1970, and the manuscript was submitted for publication on August 26, 1970.

Information in this report is embargoed under the Department of State International Traffic in Arms Regulations. This report may be released to foreign governments by departments or agencies of the U. S. Government subject to approval of the Arnold Engineering Development Center (XON), or higher authority within the Department of the Air Force. Private individuals or firms require a Department of State export license.

This technical report has been reviewed and is approved.

George F. Garey
Lt Colonel, USAF
AF Representative, PWT
Directorate of Test

Joseph R. Henry
Colonel, USAF
Director of Test

ABSTRACT

This report presents the results of an investigation to determine the transition Reynolds number characteristics of the Propulsion Wind Tunnel (16T) and the Aerodynamic Wind Tunnel (4T) by measuring the location of boundary-layer transition on a 10-deg total-angle cone. Boundary-layer thickness on the test section walls and test section noise levels were measured in an attempt to determine their influence on boundary-layer transition location. Transition Reynolds number decreased with increasing Mach number in both tunnels with a higher rate of change in Tunnel 4T. Transition Reynolds number decreased with increasing unit Reynolds number for free-stream Mach numbers ≤ 1.0 and alternated between decreasing and increasing with increasing unit Reynolds number for free-stream Mach numbers > 1.0. Test results indicated that boundary-layer transition on the cone surface was affected by test section wall angle, wall porosity, and the noise radiating from the test section walls. The boundary-layer acoustic level, as measured on the cone surface, was relatively unaffected by transition location for subsonic Mach numbers. Transition Reynolds number decreased with increasing tunnel noise level, and the sensitivity of boundary-layer transition to test section noise decreased with increasing unit Reynolds number.

CONTENTS

APPENDIX
ILLUSTRATIONS

NOMENCLATURE

a_∞	Free-stream speed of sound, ft/sec
ΔC_p	Dynamic pressure coefficient, $(\tilde{p}/q) \times 100$ percent
f	Frequency, Hz
Δf	Analyzer bandwidth, Hz
$G(f)$	Power spectral density function, $(\tilde{p})^2/\Delta f$
ℓ	Cone centerline length, 36 in.
M_∞	Test section free-stream Mach number
$p(t)$	Instantaneous, time-dependent fluctuating pressure, psf
$\tilde{p}$	Root-mean-square (rms) fluctuating pressure, $\sqrt{\overline{p(t)^2}}$, psf
p_c	Tunnel plenum pressure, reference pressure, psfa
p_p	Pitot probe pressure measured along cone surface, psfa
p_{t_∞}	Free-stream total pressure, psfa
q	Free-stream dynamic pressure, psf
Re/ft	Unit Reynolds Number, U_∞/ν_∞, 1/ft
Re_t	Transition Reynolds number, $(Re/ft)(x_t)/12$

t	Time, sec
U_∞	Free-stream velocity, ft/sec
x	Axial distance along cone surface, in.
x_t	Location of boundary-layer transition point on surface of cone, see Fig. 8, in.
α	Cone angle of attack, deg
δ_1	Representative laminar boundary-layer thickness, see Fig. 8
δ_2	Representative turbulent boundary-layer thickness, see Fig. 8
δ^*	Boundary-layer displacement thickness on the test section wall, in.
δ^*/θ	Test section wall boundary-layer shape factor
θ	Boundary-layer momentum thickness on the test section wall, in.
θ_w	Tunnel 16T east and west wall angle setting, positive angle indicates wall travel away from tunnel centerline, deg
ν_∞	Free-stream kinematic viscosity, ft^2/sec
τ	Wall porosity, percent

SECTION I
INTRODUCTION

The current trends in the development of modern high performance flight vehicles have resulted in an increased emphasis on the accuracy and validity of transonic wind tunnel testing. As a result of these trends, it has become necessary to have a better understanding of the test section flow characteristics in wind tunnels. Recent investigations in supersonic wind tunnels (Refs. 1 through 4) established an empirical relationship between transition Reynolds number and the tunnel size, tunnel wall boundary-layer noise, boundary-layer thickness, and skin friction. In contrast, a recent literature search revealed that very little information is available on transition Reynolds number and corresponding influencing factors for transonic wind tunnels.

This report presents the results of an investigation to determine the transition Reynolds number characteristics of the Propulsion Wind Tunnel (16T) and the Aerodynamic Wind Tunnel (4T) by measuring the location of boundary-layer transition on a 10-deg total-angle cone. Boundary-layer thickness on the test section walls and test section noise levels were measured in an attempt to determine their influence on transition location.

SECTION II
TEST DESCRIPTION

2.1 DESCRIPTION OF TUNNELS

2.1.1 Tunnel 16T

The AEDC Propulsion Wind Tunnel (16T) is a variable density, continuous flow tunnel capable of operation at Mach numbers from 0.20 to 1.60, and at stagnation pressures up to 4000 psfa. The test section is 16 ft square by 40 ft long and is enclosed by perforated walls of fixed 6-percent porosity. The sidewalls of the test section are movable to allow various wall angle settings as an aid in minimizing wall interference at supersonic Mach numbers. Details of the test section are shown in Fig. 1 (Appendix) and a section of the perforated walls and the geometry details of the holes are shown in Fig. 2. A more complete description of the tunnel may be found in Ref. 5.

2.1.2 Tunnel 4T

The AEDC Aerodynamic Wind Tunnel (4T) is a variable density, continuous flow tunnel and is capable of operation over a Mach number range from 0.1 to 1.3 at stagnation pressures from 300 to 3700 psfa. The test section is 4 ft square by 12.5 ft long and is equipped with variable porosity walls with an available porosity range from 0- to 10-percent open area. The sidewalls are hinged in a manner similar to Tunnel 16T. Details of the test section and the perforated walls are shown in Fig. 3. A more thorough description of Tunnel 4T may be found in Ref. 5.

2.2 APPARATUS

2.2.1 Wall Boundary-Layer and Acoustic Instrumentation

Six boundary-layer rakes were installed on the four test section walls of Tunnel 16T. Two rakes (one of 8-in. height on the bottom wall and the other of 12-in. height on the east wall) were installed at Station 0. Four rakes, each 24 in. high, were installed on each of the four walls at Station 12. The location of these rakes is shown in Fig. 1. Also, dynamic pressure transducers were installed on the west test section wall at the test section centerline height. One transducer was located forward of the perforated region at Station -10 and the other was located at Station 12 in a locally smooth region obtained by filling the adjacent wall holes. The frequency response of the transducers was flat from 100 Hz to 100 kHz but can be corrected down to 10 Hz.

Test instrumentation in Tunnel 4T consisted of a dynamic pressure transducer installed in the south test section wall at Station 88 in a locally smooth area. The transducer had a 1/8-in. diaphragm and a frequency response from 10 Hz to 10 kHz.

2.2.2 10-deg Transition Cone and Surface Pitot Probe

The geometry details of the sting-mounted 10-deg cone are shown in Fig. 4. The cone was machined from a solid piece of stainless steel. The surface was turned, heat treated, finish ground, and then polished smooth to a surface finish of 3 to 4 μin. Two flush-mounted pressure transducers were installed in the cone as shown in Fig. 4. A quick-removal mechanism was included as a part of the transducer mounting arrangement to allow for ease of replacement of a damaged transducer.

A schematic of the pitot probe and close-coupled pressure transducer showing detailed dimensions is presented in Fig. 5. The probe

was designed and fabricated for: (1) the minimization of probe-cone surface interference by the provision of a minimum probe contact area, (2) the minimization of the probe tip opening height to allow the survey of a very thin boundary layer, and (3) the minimization of pressure lag time by close-coupling the pressure transducer to maximize the probe frequency response. Considerable attention was directed to the design of the geometry of the probe support structure (particularly in the region closest to the cone) to minimize the possibility of the traversing mechanism distorting the near-field cone pressure distribution. As shown in Fig. 5, the lower portion of the support structure is inclined 60 deg from the vertical and all frontal areas were beveled and constructed as thin as was structurally possible. A nontraversing symmetrical dummy support mechanism was installed on the lower side of the cone as shown in Fig. 6. The probe traversing mechanism is driven by a d-c motor with closed-loop position control using a feedback potentiometer. A close-up view of the pitot probe on the cone surface is shown in Fig. 7.

The location of the cone in Tunnels 16T and 4T is shown in Figs. 1 and 3, respectively. The model blockage for the cone and traversing mechanism was 0.175 percent in Tunnel 16T and 2.78 percent in Tunnel 4T.

2.2.3 Data Reduction

The transition Reynolds number data from the tests in both tunnels were reduced and analyzed on line during the conduct of the test. This allowed for a more comprehensive survey in the critical areas of tunnel operation and minimized tunnel test time by improving data acquisition efficiency.

The on-line display for the transition measurements was an X-Y plotter. The X axis was driven by the output from the probe position feedback potentiometer, and the Y axis was driven by the output of the pitot probe pressure transducer. This gave an immediate display of the pressure profile, and allowed the transition location (selected on the basis of the criteria discussed in Section 3.1) to be scaled off directly. The on-line display also included the tabulation of tunnel conditions, boundary-layer profiles, and the root-mean-square (rms) outputs of the cone and wall transducers as measured by rms to d-c converters.

For off-line analysis, the outputs of the cone pressure transducers, the pitot probe transducer and position potentiometer, and the transducers on the tunnel walls were recorded on FM magnetic tape. In addition, the output of an accelerometer installed inside the cone to evaluate the structural vibration input to the transducers was recorded.

3

The cone and wall data were analyzed using an analog-type, constant bandwidth, frequency analyzer. The analysis was divided into two frequency ranges. The first covered the range from 10 Hz to 10 kHz and was intended to investigate the far field or the overall tunnel environment. The second covered the range from essentially 0 to 100 Hz and was intended to investigate the near-field effects of transition.

2.3 TEST PROCEDURE

The cone surface pressure surveys were conducted while holding free-stream Mach number constant and varying total pressure. In order to avoid the possibility of model interference from the two forward boundary-layer rakes, in Tunnel 16T, boundary-layer data for the test section wall at Station 0 were obtained first and then the pitot rakes were removed before commencing with the transition measurements.

It was determined that there were slight differences in the pressure profile along the cone surface when traversing the pitot probe aft to forward and forward to aft. These differences could be diminished but not eliminated by reducing the traversing speed of the probe, and are attributed to the probe response time and a possible hysteresis effect on the cone boundary layer by the traversing pitot probe. As a result of this occurrence, all pressure profiles were obtained by traversing the pitot probe from an aft to a forward position. With Mach number held constant, and at a minimum total pressure for which transition could be detected, pressure profiles were obtained for incremental changes in tunnel total pressure until the pitot probe sensitivity diminished and transition could no longer be detected.

In Tunnel 16T the Mach number was varied from 0.6 to 1.3 in 0.05 increments or less. In the critical Mach number range $0.65 \leq M_\infty \leq 0.80$, as defined in Ref. 6, the increment was either 0.02 or 0.03. Unit Reynolds number was varied from less than 1.5 million to greater than 4.0 million. In addition, the influence of test section wall angle, flow angularity (by varying cone angle of attack), and compressor stator blade angle was evaluated.

In Tunnel 4T the Mach number was varied from 0.3 to 1.3 in increments of 0.10 or less. The unit Reynolds number range was approximately the same as in Tunnel 16T. Wall porosity was varied from 0 to 10 percent. Test section wall angle and cone angle of attack were not varied in Tunnel 4T.

2.4 PRECISION OF MEASUREMENTS

The estimates of the errors in the steady-state data as determined from instrumentation and calibration inaccuracies are as follows:

Parameter	Accuracy
M_∞	±0.002
p_{t_∞}	±4 psfa
α	±0.03 deg
θ_w	±0.03 deg
τ	±0.02 percent
x	±0.10 in.

The accuracy of the tabulated on-line rms data as measured by the pressure transducers is estimated to be ±0.4 db, or ±2.0 psf at a sound pressure level of 160 db. These estimates are based on a confidence level of 95 percent.

The uncertainty of the frequency analysis based on a 67-percent confidence level was established as follows:

From 30 to 500 Hz	11.1 percent
From 500 Hz to 10 kHz	3.53 percent

SECTION III
TRANSITION DETECTION TECHNIQUES

3.1 GENERAL

A pictorial description of a typical boundary-layer buildup from laminar flow through a transition region to turbulent flow is shown in Fig. 8. The line that defines the boundary layer is the boundary-layer thickness, δ, as shown in the inset. This line can also be considered as the point at which the local velocity reaches the free-stream velocity. When moving downstream, the laminar region is characterized by a gradually increasing surface temperature, a negative pitot pressure gradient, and very low-level pressure fluctuations. The transition region is characterized by a sharp increase in surface temperature, a positive pitot pressure gradient, and an increase in the level of the fluctuating pressures at low frequencies. The turbulent region is characterized by a relatively constant surface temperature, a small negative pitot pressure gradient, and as the turbulent boundary layer builds up, an increase in the level of the pressure fluctuations at all frequencies.

3.2 SURFACE STEADY-STATE PITOT PRESSURE

Steady-state pressure profiles that were obtained in Tunnel 4T at $M_\infty = 0.80$ using the pitot probe are presented in Fig. 9. These profiles are typical of those obtained in both Tunnels 4T and 16T throughout the Mach number and Reynolds number range. It is emphasized that these are steady-state or d-c pressure profiles and that the dynamic or fluctuating component has been filtered out.

The location of the boundary-layer transition on the cone surface was chosen as the peak in the steady-state pitot pressure profile as depicted in Fig. 9. The location of this peak is generally accepted as being near the end of the boundary-layer transition region. The beginning of the transition region is generally considered to be in the neighborhood of the minimum pressure. The location of the minimum pressure is quite difficult to determine, however, particularly at the higher Reynolds numbers.

It was discovered that the size of the pitot probe relative to the cone surface boundary-layer thickness was a determining factor in the effectiveness of the probe in detecting the location of transition. Figure 8 shows a pictorial description of the pitot probe size in relationship to an assumed cone boundary-layer thickness. As the probe moves forward on the cone surface from the turbulent to the laminar region, the probe senses an increasing total pressure with decreasing turbulent boundary-layer thickness, a sudden drop in total pressure associated with transition, and finally again an increasing total pressure with decreasing thickness of the laminar boundary layer. As unit Reynolds number is increased, the transition location moves forward on the cone surface into a correspondingly decreasing boundary-layer thickness. A limiting condition is eventually reached where the surface pitot probe cannot measure the small change in total pressure that occurs in the transition region because of the large ratio of probe tip height to boundary-layer thickness.

3.3 SURFACE RMS PITOT PRESSURE

With the inherent limitation of the probe in mind, the feasibility of using the fluctuating pressure rather than a steady-state pressure response as a detection technique was investigated during the Tunnel 4T test. It is a well-known fact that the transition region is characterized by an increase in the level of pressure fluctuations in the lower frequency range. This fact was confirmed by the unfiltered plot of the rms pressure profile using the X-Y recorder. The technique consisted of using

an R-C-coupled rms voltmeter to measure the rms output of the probe pressure transducer in the frequency range from 2 Hz to the cutoff frequency of the probe, which was approximately 50 Hz. The rms level was converted to a proportional d-c level and recorded versus probe position on a second X-Y plotter. Typical rms pressure profiles are shown in Fig. 10 and compared with unfiltered steady-state pressure profiles. The steady-state pressure profiles indicate the very low frequency fluctuations in the transition region that were discussed previously. Note that the rms pressure profiles reveal a well-defined peak in an area roughly defined as between the center of the transition region and the minimum in the steady-state pressure profiles. The point of primary significance, however, is that the rms peak exhibits excellent resolution for the higher Reynolds numbers.

There was one basic limitation to the rms detection technique that precluded its use for this current study. This limitation was essentially a dynamic pressure lag error which is similar to a static pressure lag error. It is reasonable to conclude that this dynamic error is the reason that the rms peak did not occur at a more central location in the transition region as was expected. To eliminate this dynamic skew error, a probe with a close-coupled, subminiature transducer will have to be designed, and a reduction in the traversing rates will be required. It has been demonstrated, however, that the technique has sufficient merit to justify further study.

SECTION IV
RESULTS AND DISCUSSION

4.1 TEST SECTION WALL BOUNDARY-LAYER CHARACTERISTICS IN TUNNEL 16T

The variation of the boundary-layer parameters, δ^* and θ, with unit Reynolds number at Station 12 (see Fig. 1) for the east and bottom test section wall for a wall angle of 0 deg is presented in Fig. 11. The effect of wall angle, θ_w, on δ^* and θ at Station 12, and for Mach numbers greater than 1.0 is presented in Fig. 12. Data obtained for the north and top test section walls at Station 12 indicated that symmetry in the boundary-layer parameters did exist between opposing test section walls. The boundary-layer parameters obtained for the east and bottom test section wall at Station 0, although of slightly smaller magnitude, showed the same trends as those at Station 12. The figures show that the boundary-layer parameters were invariant with changes in unit Reynolds number and show an increase in magnitude of the parameters as the sidewalls

were diverged. The east wall exhibited a slightly greater magnitude of the boundary-layer parameters for all wall angles throughout the Mach number range similar to that shown in Fig. 13 at Station 12, and for 0-deg wall angle. Figure 13 shows also that the magnitude of δ^* and θ gradually decreased with increasing Mach number up to a Mach number near 1.05 and then gradually increased with increasing Mach number. The magnitude of the shape factor, δ^*/θ, gradually increased with increasing Mach number throughout the Mach number range.

4.2 TRANSITION

The variation of the nondimensionalized transition location, x_t/ℓ, with unit Reynolds number and with free-stream Mach number for Tunnels 16T and 4T is shown in Fig. 14. Wall porosity is fixed at 6.0 percent in 16T and set at 6.0 percent in 4T. Also presented in Fig. 14 are the effects of varying Tunnel 16T test section wall angle on transition location. The most forward transition location for which data are presented generally represents the limiting Reynolds number for which transition could still be determined as described in Section 3.2. In general, a study of Fig. 14 reveals that (1) transition location varies logarithmically with unit Reynolds number for both tunnels in the Reynolds number range of this test; (2) diverging the test section wall angle in Tunnel 16T caused the transition location to move aft on the cone; and (3) the transition location was farther aft in Tunnel 16T than in Tunnel 4T, although the difference decreased with increasing unit Reynolds number.

A comparison of transition location obtained for the 6-percent test section wall porosity setting and at settings considered optimum for wave cancellation in Tunnel 4T is presented in Fig. 15 for Mach numbers 1.0 and above. The available test time did not permit a systematic investigation of the effects of wall porosity on transition. However, trends in the data of Fig. 15 indicate that transition location in general probably moves forward with increasing wall porosity.

No attempt was made to measure or correct the angle of attack of the cone caused by flow angularity. Transition data were obtained for a cone angle-of-attack range from -1 to 1 deg in Tunnel 16T at Mach number 0.80 and a unit Reynolds number of 3.35 million to determine the sensitivity of transition location to flow angularity. These data are presented in Fig. 16 and exhibit a fairly linear variation of transition location with angle of attack up to 1/2 deg where a reverse trend occurs with further increase in angle of attack. Assuming that flow angularity would fall within the range of ±1/2 deg, the error in transition location would fall within the range of ±0.72 in. per degree of flow angularity.

The best fit straight lines that are shown in Fig. 14 were used to determine the variation of the transition location with Mach number for three different fixed unit Reynolds numbers as shown in Fig. 17. In General, the transition location moved forward with increasing Mach number in both tunnels with a faster rate of change indicated in Tunnel 4T.

The variation of transition Reynolds number with unit Reynolds number is shown in Figs. 18 and 19 for Tunnels 16T and 4T, respectively. Both tunnels exhibited a negative slope of the characteristic curves for $M_\infty \leq 1.0$. For $M_\infty > 1.0$, the slope alternates between positive and negative for different Mach numbers. In contrast, the results of Ref. 2 indicated that the slope was always positive for supersonic Mach numbers.

4.3 ACOUSTIC CHARACTERISTICS

The acoustic noise levels measured on the surface of the 10-deg cone can be influenced by either of two sources: one, the far-field pressure disturbances that are controlled by the test section walls and tunnel flow noise, and two, the near-field pressure disturbances that are controlled by the cone boundary-layer characteristics. To evaluate the acoustic measurements, it is necessary to isolate the source or sources that are controlling the overall rms noise levels. This can be done by a comparison of the overall levels and also the frequency spectra as measured by the two cone transducers relative to the location of the transition region. The acoustic data presented and discussed in the sequel were taken with the pitot probe in the fully retracted position. This was necessary since it was determined that the noise levels measured on the cone surface varied with probe position when the probe was extended.

In an attempt to isolate the disturbances generated by boundary-layer transition from those generated by tunnel noise, the overall rms noise levels measured in Tunnel 16T at the two transducer positions on the cone are plotted and correlated with transition location as shown in Figs. 20 and 21. A study of Figs. 20 and 21 reveals that when the noise levels are low (i. e., $\Delta C_p = 1.0$ percent for $M_\infty \geq 1.0$) the overall levels are slightly higher in the transition region. When the noise levels are high (i. e., $\Delta C_p > 1.0$ percent and $M_\infty < 1.0$) the overall levels are relatively invariant with transition location.

A representative comparison of the differences in the frequency spectra relative to transition location for $M_\infty = 0.75$ and 1.10 is shown in Figs. 22 and 23, respectively. In general, for subsonic Mach numbers, and because of the predominately high level in the 600- to 700-Hz

band, the level of the frequency spectra at frequencies above 600 Hz, as measured by both the forward and aft transducers, was invariant with transition location. For supersonic Mach numbers the level of the spectra was invariant above 2000 Hz. A comparison of the spectra at the lower frequencies indicates that the noise levels in the transition region are higher than the levels behind the transition region. Unfortunately, a comparison of the spectra in the region forward of transition is not available. As expected, when the transition location was forward of both transducers, the noise levels measured by both transducers were identical throughout the frequency spectra.

Based on this analysis it appears that the use of a low frequency bandpass filter on the output of the cone transducers should enable the detection of the location of transition. Further, if the location of transition is not known and the overall noise levels are such that $\Delta C_p \geq 1.0$ percent, then the free-stream acoustic levels measured on a 10-deg cone are best represented by the most aft transducer or the one most likely to be always in the turbulent boundary layer. If the transition location is known, however, a transducer location forward of the transition region or in the laminar boundary layer is preferable for measurements of flow noise.

A comparison of the noise levels in the two tunnels is shown in Fig. 24. Note that the levels are higher in Tunnel 16T for subsonic Mach numbers and in Tunnel 4T for supersonic Mach numbers.

4.4 CORRELATION OF TRANSITION AND NOISE

It has been shown in Ref. 2 that in supersonic tunnels the radiated noise from the test section wall boundary layer affects the transition Reynolds number. It is of considerable interest to determine if a similar cause and effect relationship exists in transonic tunnels. Although the test objectives in Tunnels 16T and 4T were not intended to specifically isolate the influence of noise on transition, the noise levels were measured simultaneously with the measurement of the location of boundary-layer transition. Thus, since it was concluded in Section 4.3 that the overall rms levels measured on the 10-deg cone were controlled by the tunnel noise (both wall and free-stream), it should be possible to show an indirect correlation of noise and transition, if such a correlation exists.

The variation of transition Reynolds number with noise level is obtained by cross plotting the variation of transition Reynolds number with Mach number for fixed unit Reynolds number, and the variation of noise level (nondimensionalized by total pressure in this case) with Mach number

for the same unit Reynolds numbers. The results of analyzing the data in this manner are shown in Fig. 25. The curves represent the best fit of the interpolated data points and reflect the general trends over the Mach number range from 0.60 to 1.00. Note that in both tunnels there is a corresponding decrease in transition Reynolds number with increasing noise levels. Note also that the Tunnel 16T noise level-transition Reynolds number characteristic shows an inverse dependence on unit Reynolds number, whereas Tunnel 4T characteristics are relatively invariant. In both tunnels, however, the slope tends towards zero as unit Reynolds number is increased. This fact indicates that the sensitivity of transition to test section noise decreases with increasing unit Reynolds number.

There is definite indication shown in Fig. 25 of a dependence of transition Reynolds number in a given tunnel on test section noise levels. When comparing tunnels, however, the level of Re_t in Tunnel 16T is higher than in Tunnel 4T even though the noise level is also higher. Although this appears to contradict the previously reached conclusion on the transition versus noise correlation, it is felt that this difference can be attributed to differences in turbulence levels or test section size.

In Tunnel 16T, the compressor stator blade angle is used for primary control of subsonic Mach numbers. With the use of plenum suction, it is possible to change the blade angle by a slight amount, and still maintain the same test section conditions. The effect of varying the stator blade angle for a number of subsonic Mach numbers was detected by a well-defined shift in the frequency spectra as measured on the 10-deg cone. There was no change in the transition location, however, and no correlation was found between transition and blade angle.

The foregoing analysis and discussion of the correlation of noise and transition are limited by the fact that the evaluation of the relative turbulence levels was not included and also by the fact that a change in the noise levels was accompanied by a change in the tunnel operating conditions. Future studies should include instrumentation to measure the turbulence levels as well as the noise levels and equipment to generate a pure acoustic disturbance in the test section.

SECTION V
CONCLUDING REMARKS

The transition Reynolds number and acoustic characteristics have been measured in Tunnels 16T and 4T using a 10-deg cone. In addition,

the wall boundary-layer characteristics were measured in Tunnel 16T. Based on an analysis of the results of these measurements, the following conclusions were reached:

1. Boundary-layer transition location on the 10-deg cone varied logarithmically with unit Reynolds number.

2. Diverging the test section wall angle (increasing test section wall boundary-layer thickness) in Tunnel 16T caused the transition location on the cone to move aft.

3. The boundary-layer transition location was farther aft in Tunnel 16T although the differences between the two tunnels decreased with increasing Reynolds number.

4. Trends indicated that the transition location on the cone in Tunnel 4T tended to move forward with increasing wall porosity.

5. Transition Reynolds number decreased with increasing Mach number in both Tunnels 4T and 16T with Tunnel 4T indicating a higher rate of change.

6. Transition Reynolds number decreased with increasing unit Reynolds number for $M_\infty \leq 1.0$ and alternated between decreasing and increasing for $M_\infty > 1.0$.

7. The boundary-layer acoustic level, as measured on the cone surface, is relatively unaffected by transition location for subsonic Mach numbers.

8. Both Tunnels 4T and 16T exhibited a decrease in transition Reynolds number with increasing noise level.

9. The sensitivity of transition to test section noise decreased with increasing unit Reynolds number.

REFERENCES

1. Pate, S. R. "Measurements and Correlations of Transition Reynolds Numbers on Sharp Slender Cones at High Speeds." AEDC-TR-69-172 (AD698326), December 1969.

2. Pate, S. R. and Schueler, C. J. "Effects of Radiated Aerodynamic Noise on Model Boundary-Layer Transition in Supersonic and Hypersonic Wind Tunnels." AEDC-TR-67-236, March 1968. Also AIAA Paper 68-375.

3. Pate, S. R. and Brown, M. D. "Acoustic Measurements in Supersonic Transitional Boundary Layers." AEDC-TR-69-182 (AD694071), October 1969.

4. Baker, W. B., Jr. and Pate, S. R. "Measurement of the Transition Reynolds Number in the AEDC 16-Ft Supersonic Propulsion Wind Tunnel." AEDC-TR-67-144 (AD817165), July 1967.

5. Test Facilities Handbook (Eighth Edition). "Propulsion Wind Tunnel Facility, Vol. 5." Arnold Engineering Development Center, December 1969 (AD863646).

6. Credle, O. P. and Shadow, T. O. "Evaluation of the Overall Root-Mean-Square Fluctuating Pressure Levels in the AEDC PWT 16-Ft Transonic Tunnel." AEDC-TR-70-7 (AD864827), February 1970.

APPENDIX
ILLUSTRATIONS

EAST
WALL

| 12

TYPICAL
BOUNDARY
LAYER RAKE
LOCATION

B

SECTION A-A

PRESSURE
TRANSDUCER

EAST
WALL

24 (Typ.)

24 (Typ.)

SECTION B-B

BOTTOM WALL

A

SOLID
AREA

B

PERFORATED
WALLS

SOLID DIVERGED WALL SECTION
TO ALLEVIATE STRUT BLOCKAGE

MODEL SUPPORT
STRUT

¢

| STA | STA | STA. | STA. | STA. | STA. |
| -10 | 0 | 5.45 | 12 | 28 | 40 |

A   A   B

ALL DIMENSIONS IN INCHES AND TUNNEL STATIONS IN FEET
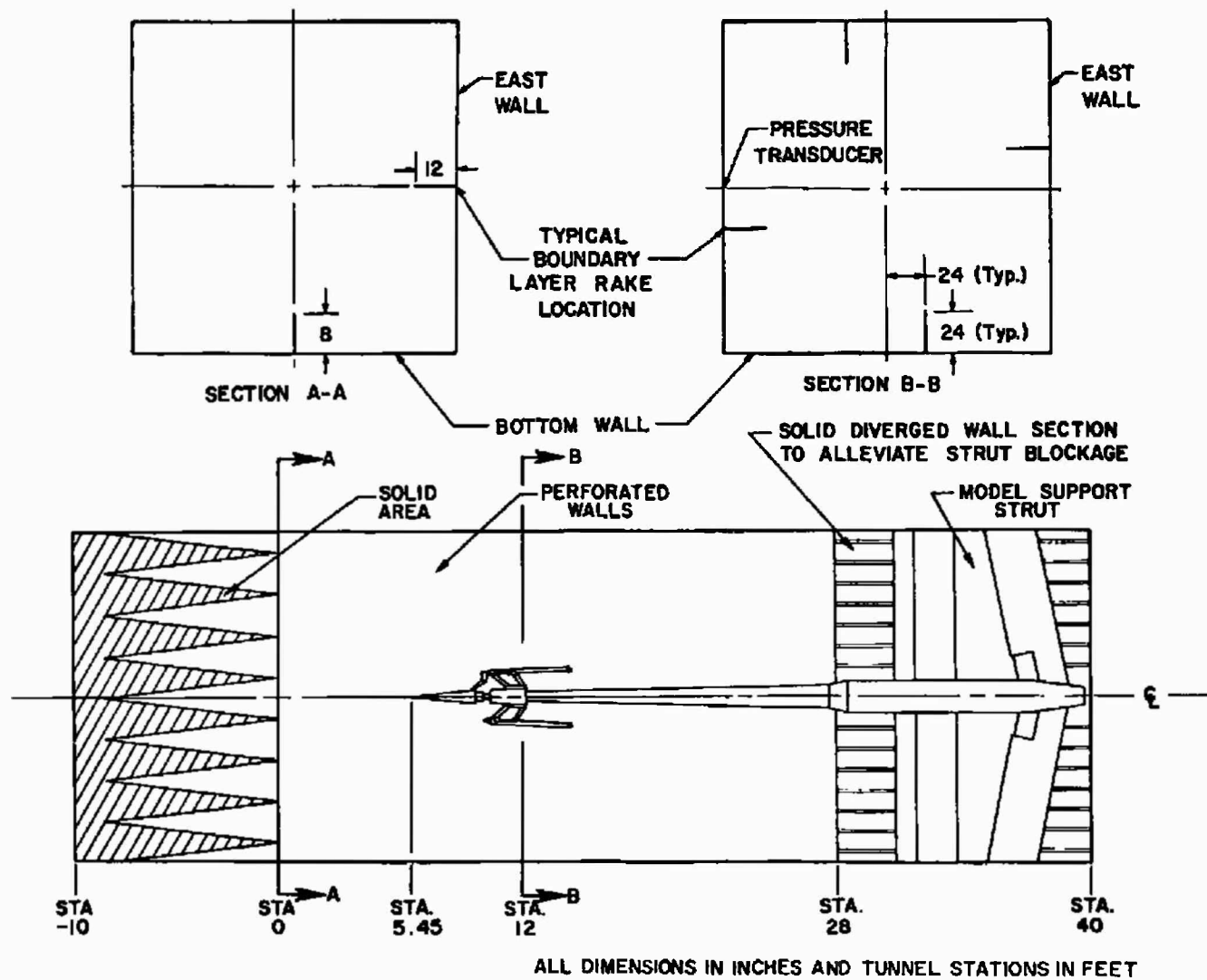
Fig. 1 Location of 10-deg Transition Cone and Wall Mounted Instrumentation in Tunnel 16T
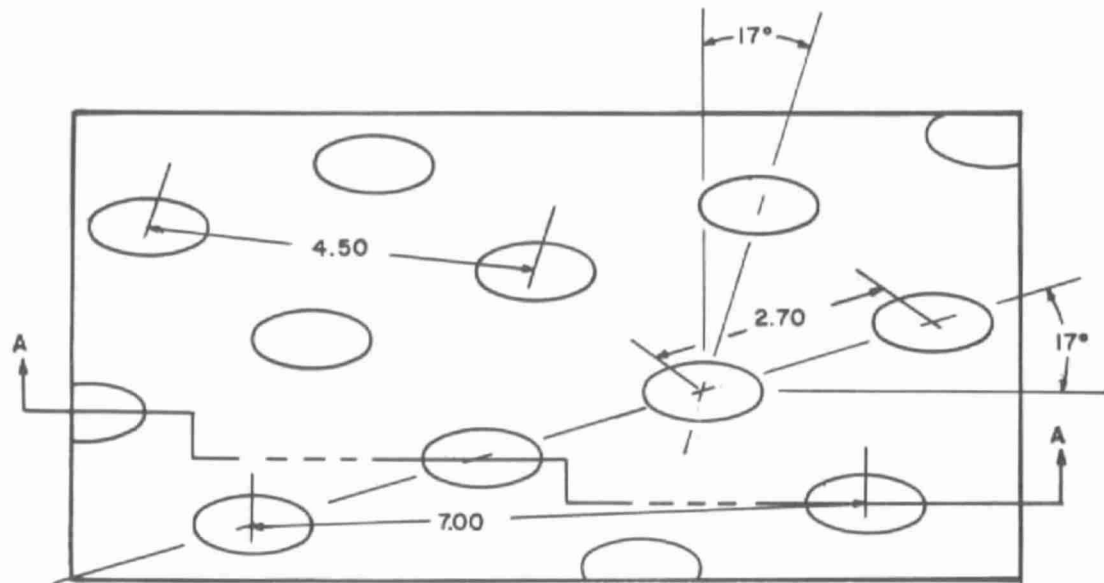
TYPICAL PERFORATED WALL PATTERN

ALL DIMENSIONS IN INCHES
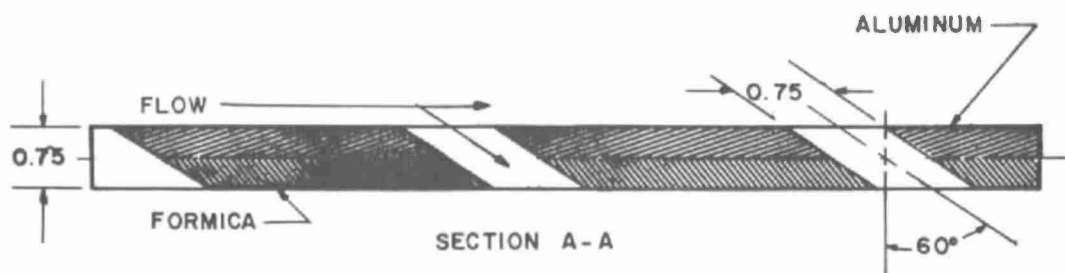
Fig. 2 Details of Tunnel 16T Perforated Test Section Walls

AIR FLOW

60°

3.75

0.500 DIA.

AIRSTREAM SURFACE

0.375

0.375
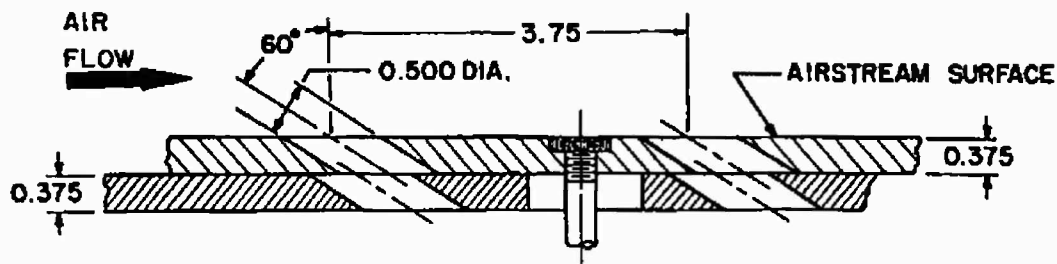
TYPICAL PERFORATED WALL CROSS SECTION

SOLID AREAS

PERFORATED WALLS (10 % MAXIMUM OPEN AREA)

FLOW
EXPANSION
REGION

STA.
0.0

STA.
36.0

STA.
84.61

STA.
88.0

STA.
150.0

TRANSDUCER
LOCATION
SOUTH WALL ₵

TUNNEL STATIONS IN INCHES
ALL DIMENSIONS IN INCHES
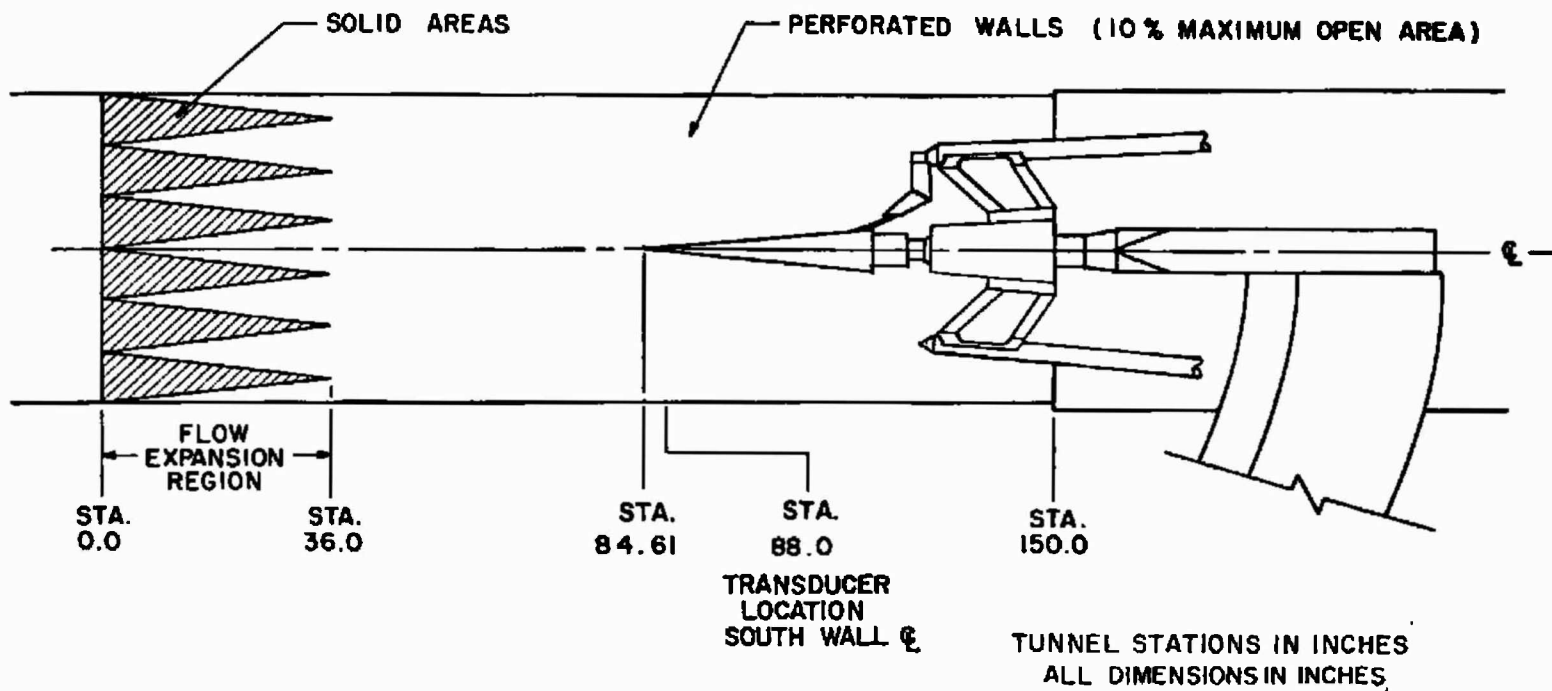
Fig. 3 Details of 10-deg Transition Cone Installation and Perforated Test Section Walls
in Tunnel 4T

REFERENCE CAVITY

REFERENCE TUBE TO
PLENUM PRESSURE

POWER AND SIGNAL CABLES

1/8 PRESSURE TRANSDUCER

0.50
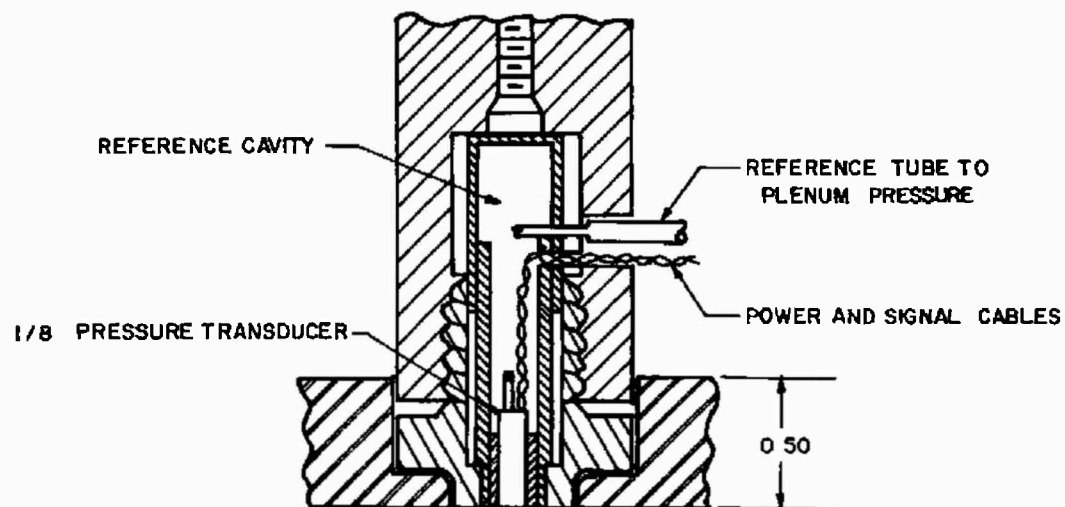
DETAIL OF TRANSDUCER
INSTALLATION (TYP)

ALL DIMENSIONS IN INCHES

SURFACE FINISH = 3 MICRONS

0°

TIP RADIUS
0.005

LOCATION OF TRAVERSING PITOT PROBE

10°

X_1

X_2

225°

180°

X_1

X_2

FRONT VIEW

18

26

36

5.25

6.30

5.00
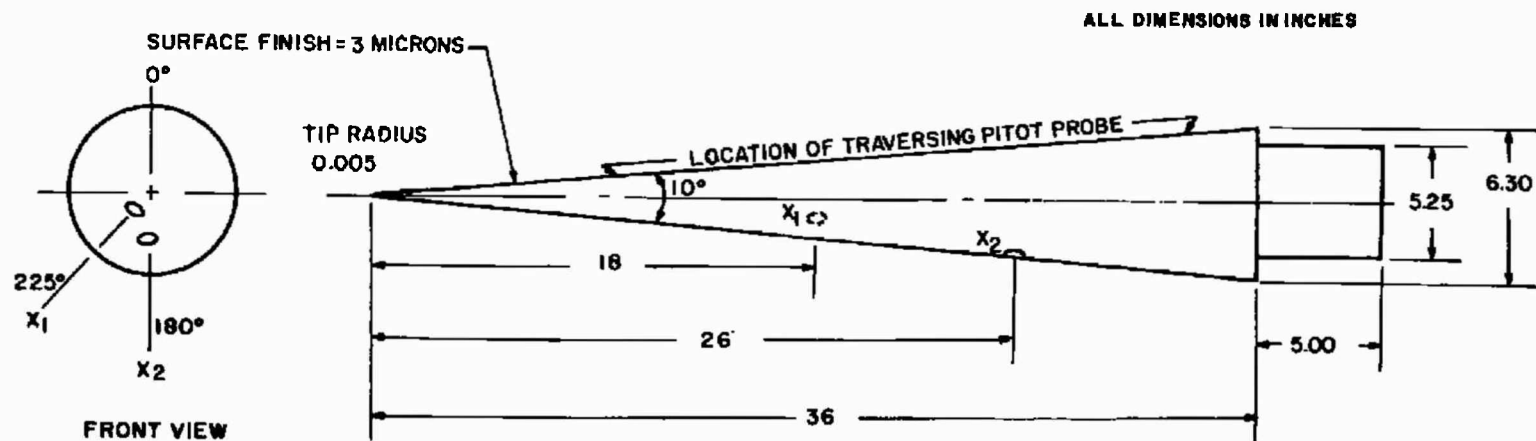
Fig. 4 Details of 10-deg Transition Cone and Mounting Arrangement for Pressure Transducers
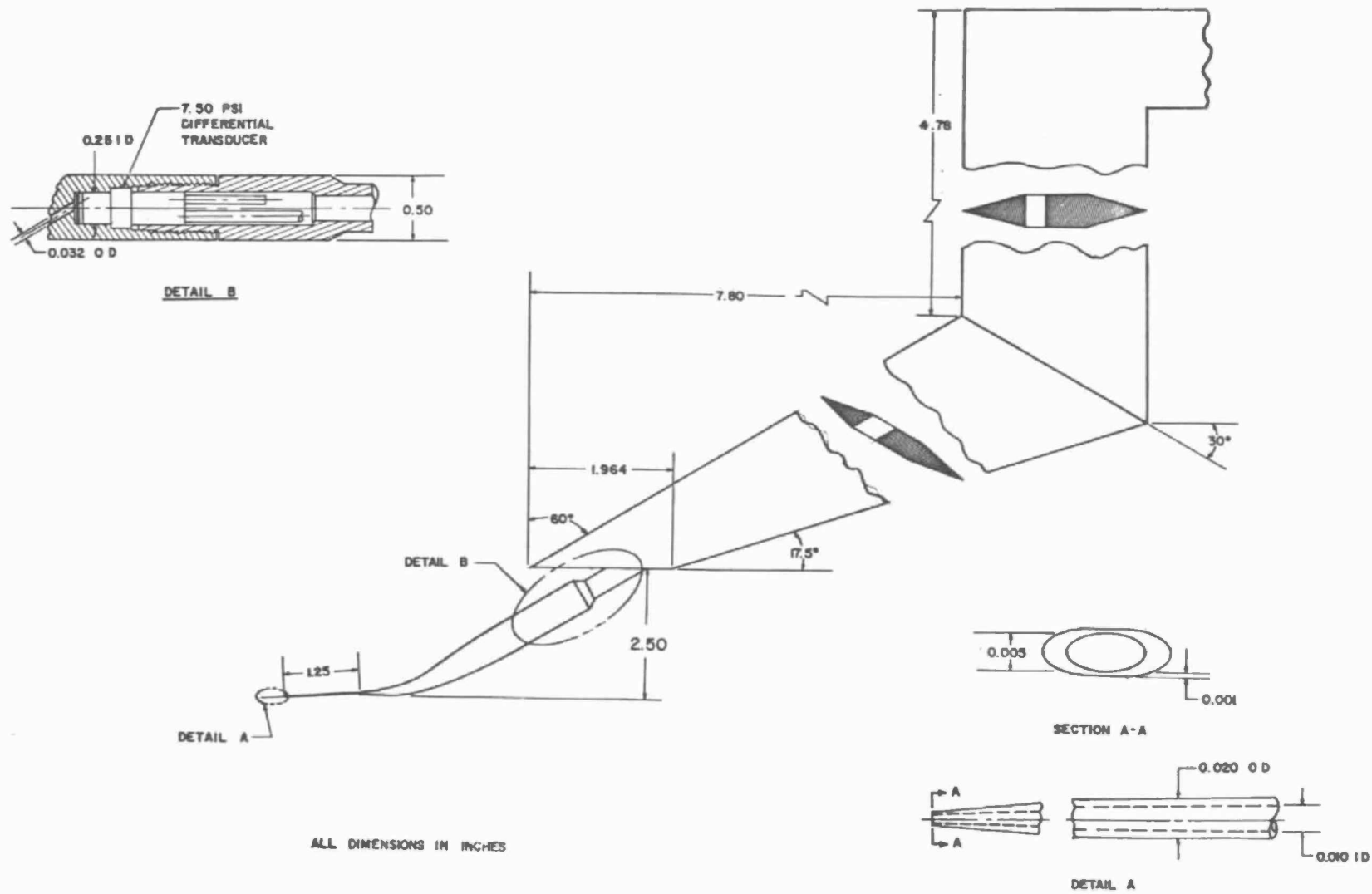
Fig. 5 Details of Traversing Pitot Probe (and Strut) and Probe Pressure Transducer Installation
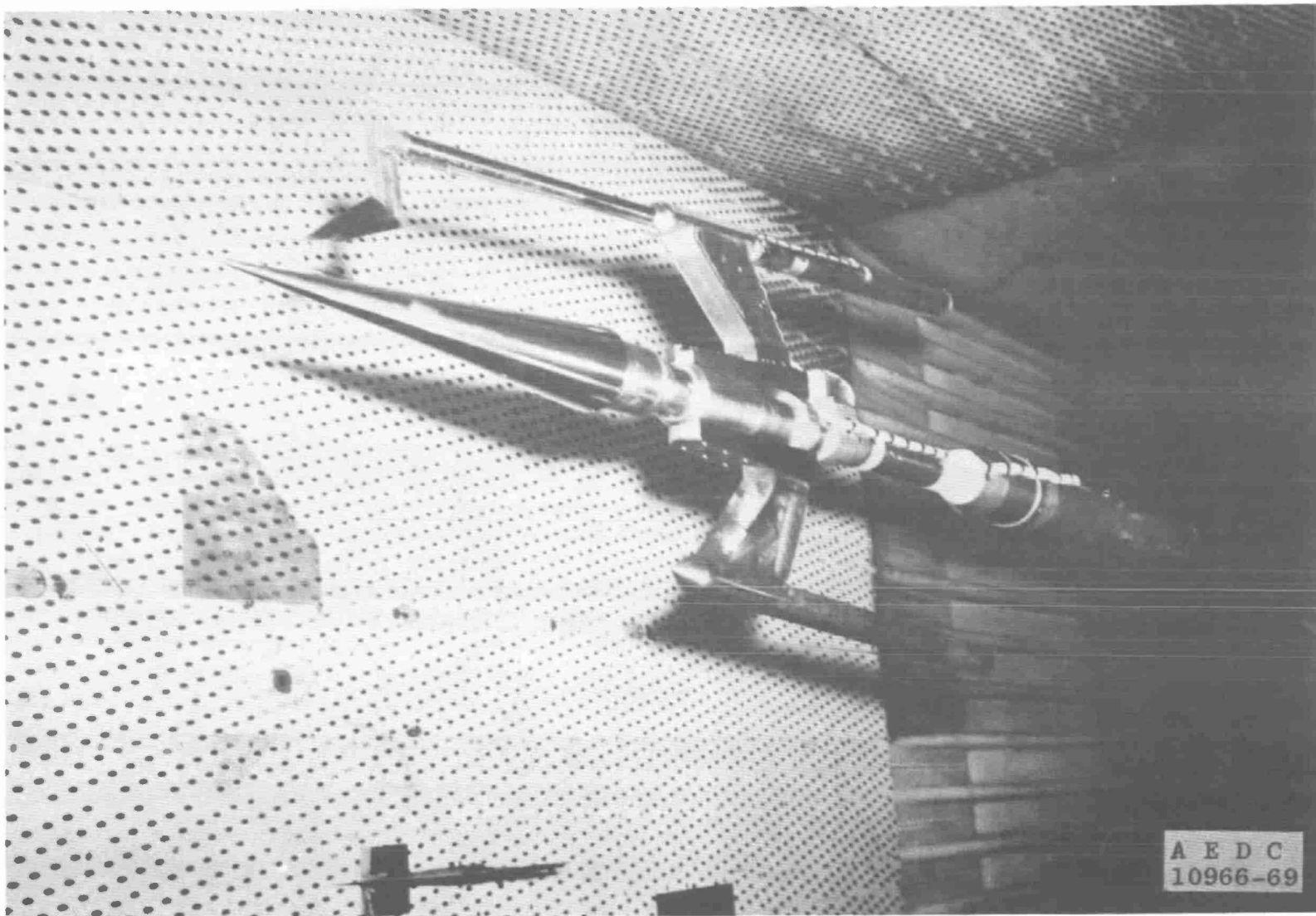
Fig. 6 Photograph of 10-deg Transition Cone Installed in Tunnel 16T
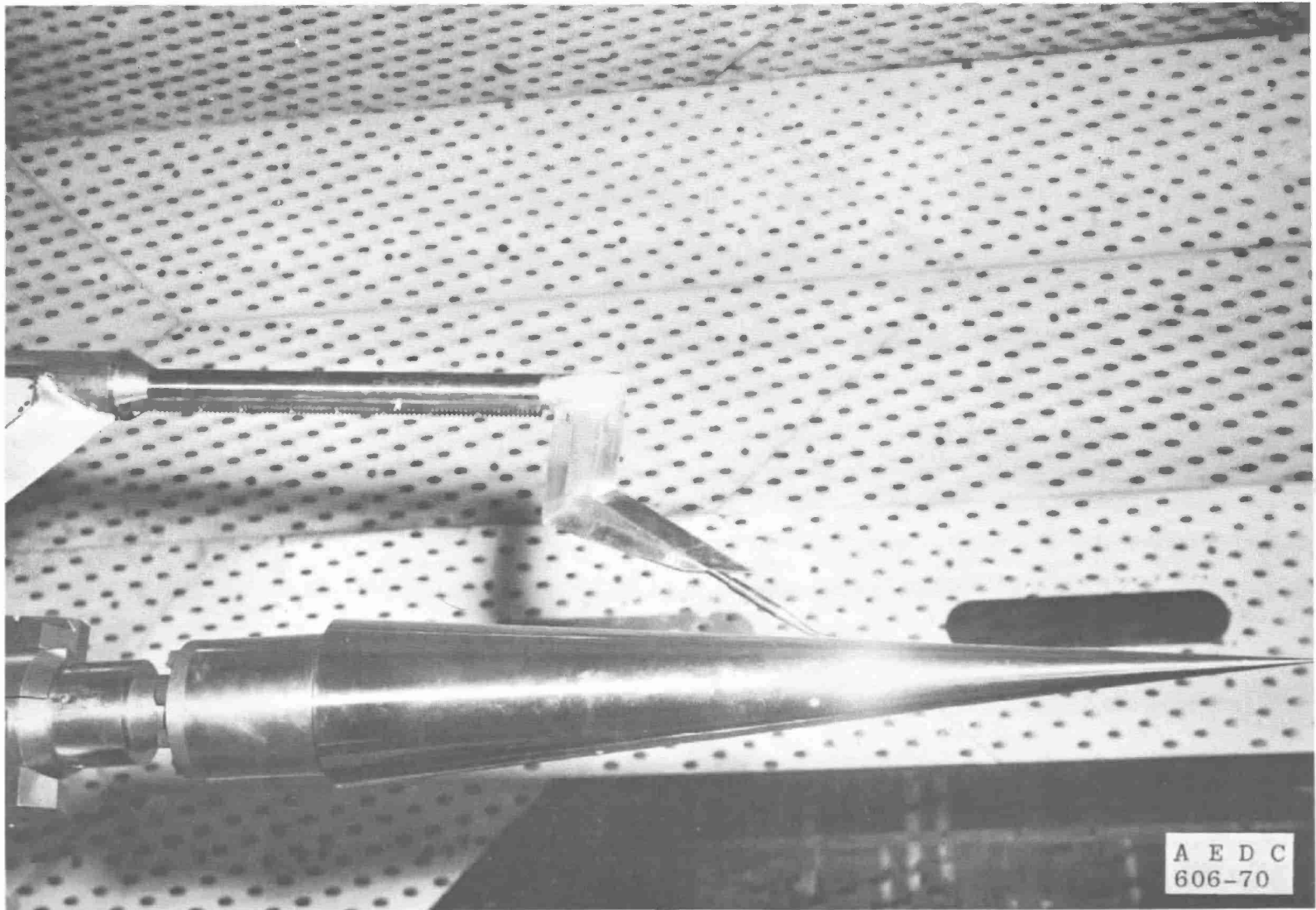
Fig. 7 Photograph of 10-deg Transition Cone and Traversing Pitot Probe
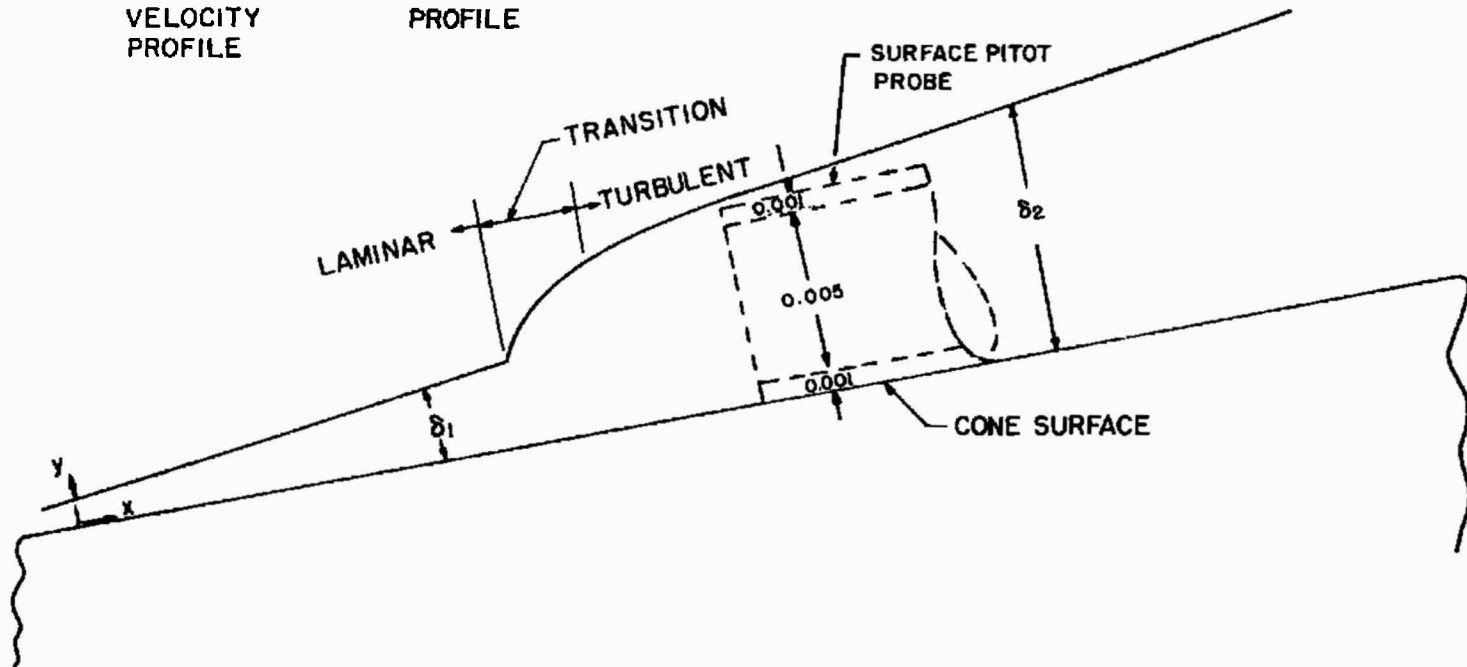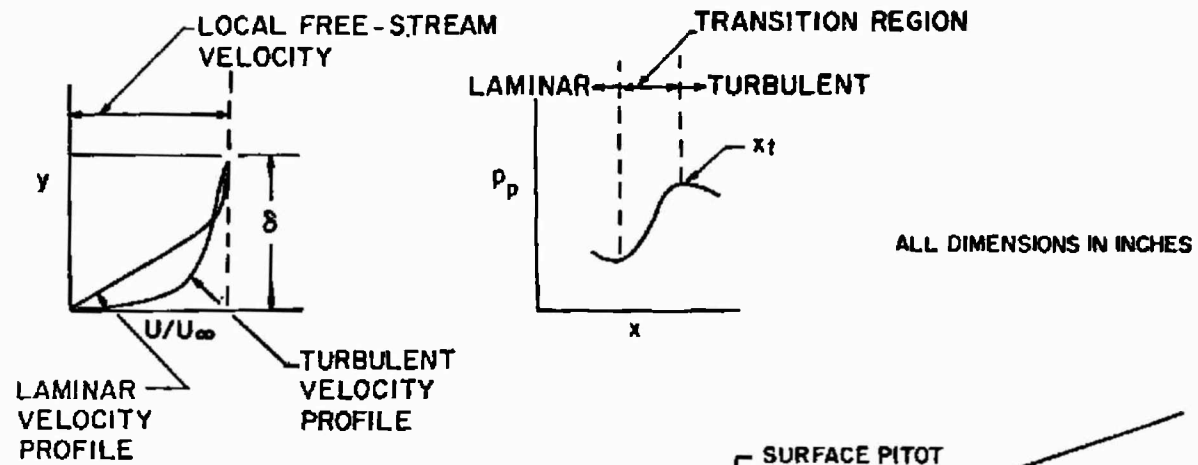
Fig. 8 Pictorial Description of a Typical Boundary-Layer Buildup
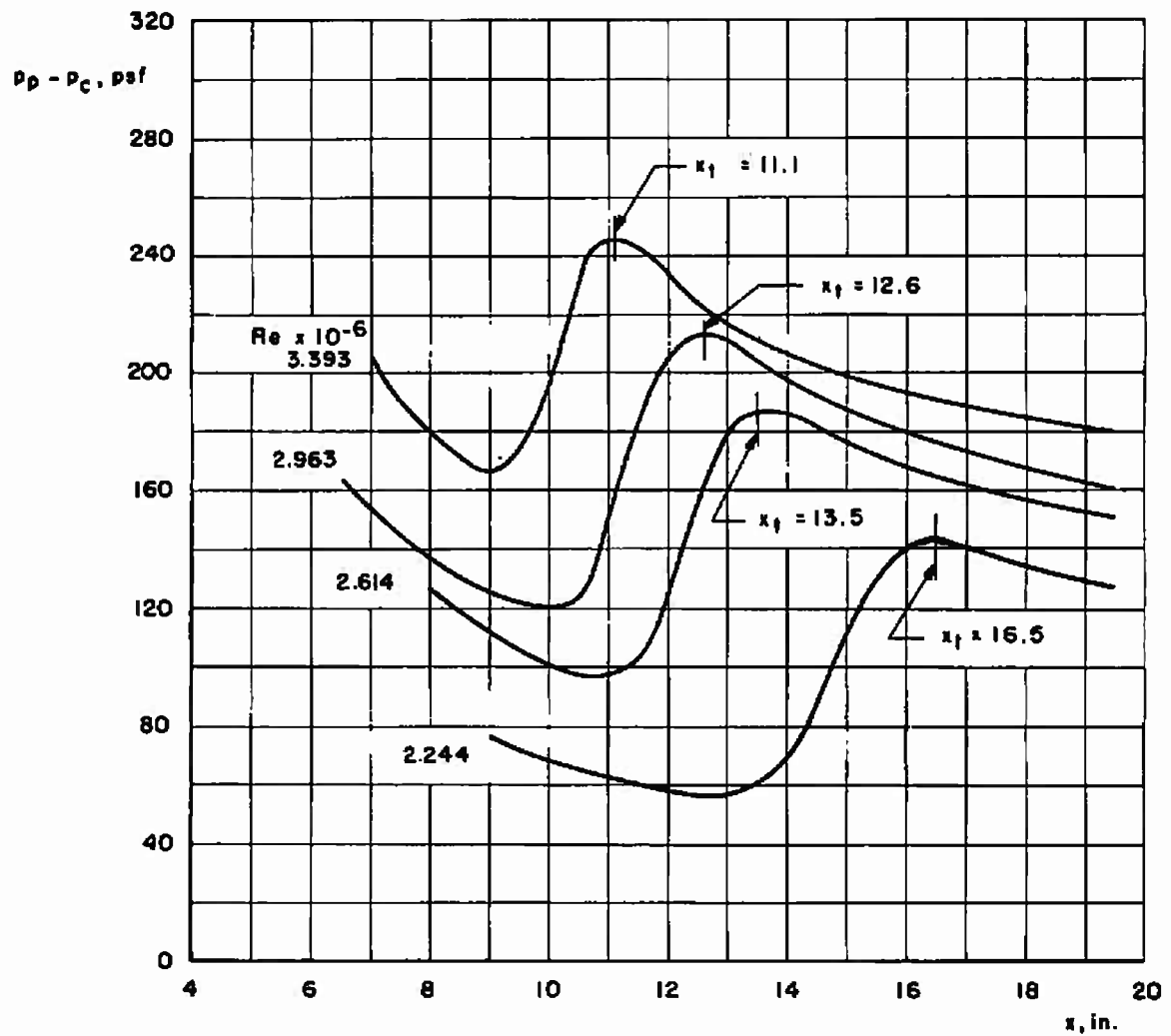
Fig. 9 Typical Profile of Steady-State Pitot Surface Pressure
versus Position on Cone for Tunnel 4T, M$_\infty$ = 0.80
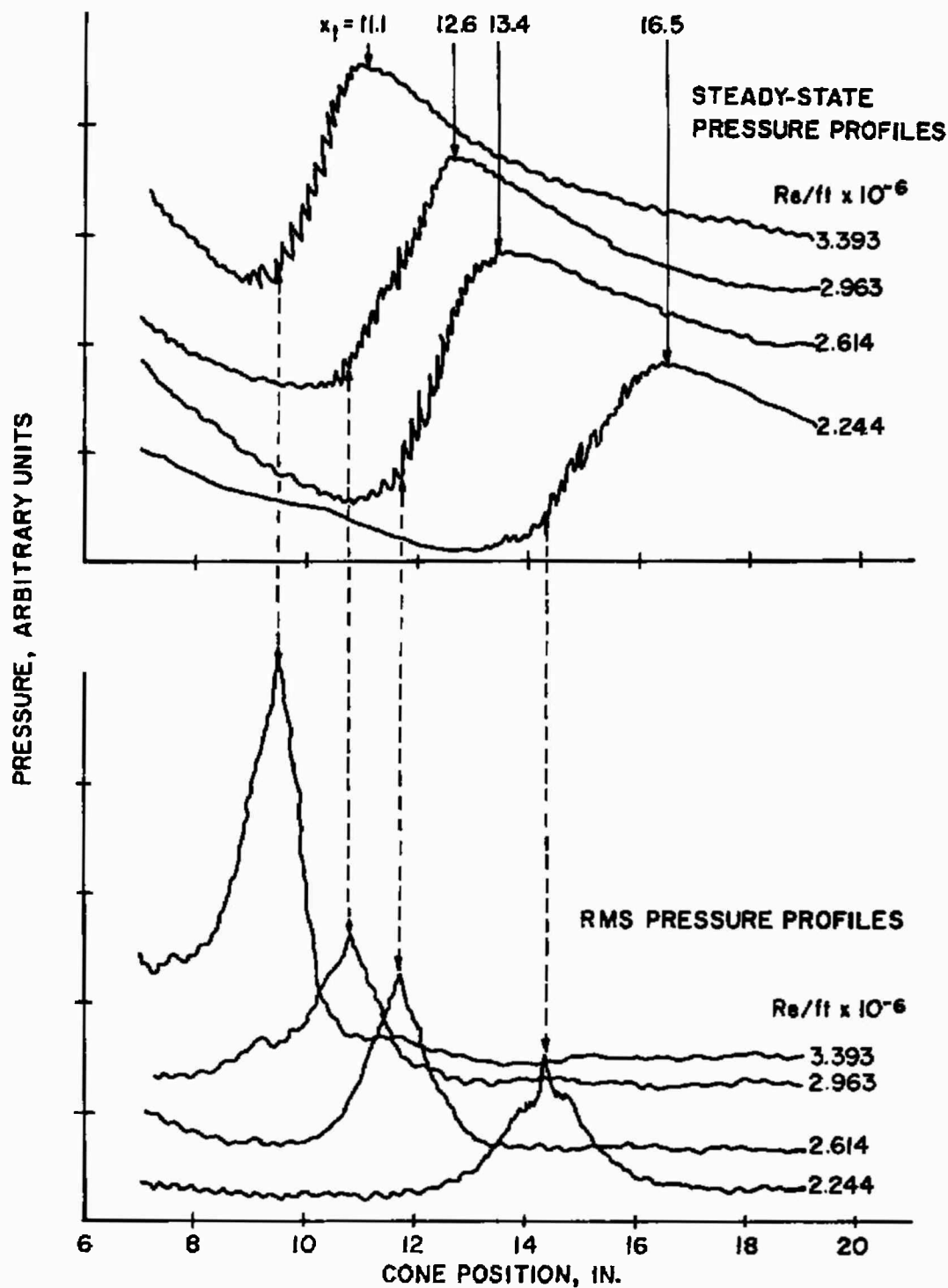
a. $M_\infty = 0.80$

Fig. 10 Comparison of Pitot Probe Steady-State and rms Pressure Profiles, Tunnel 4T
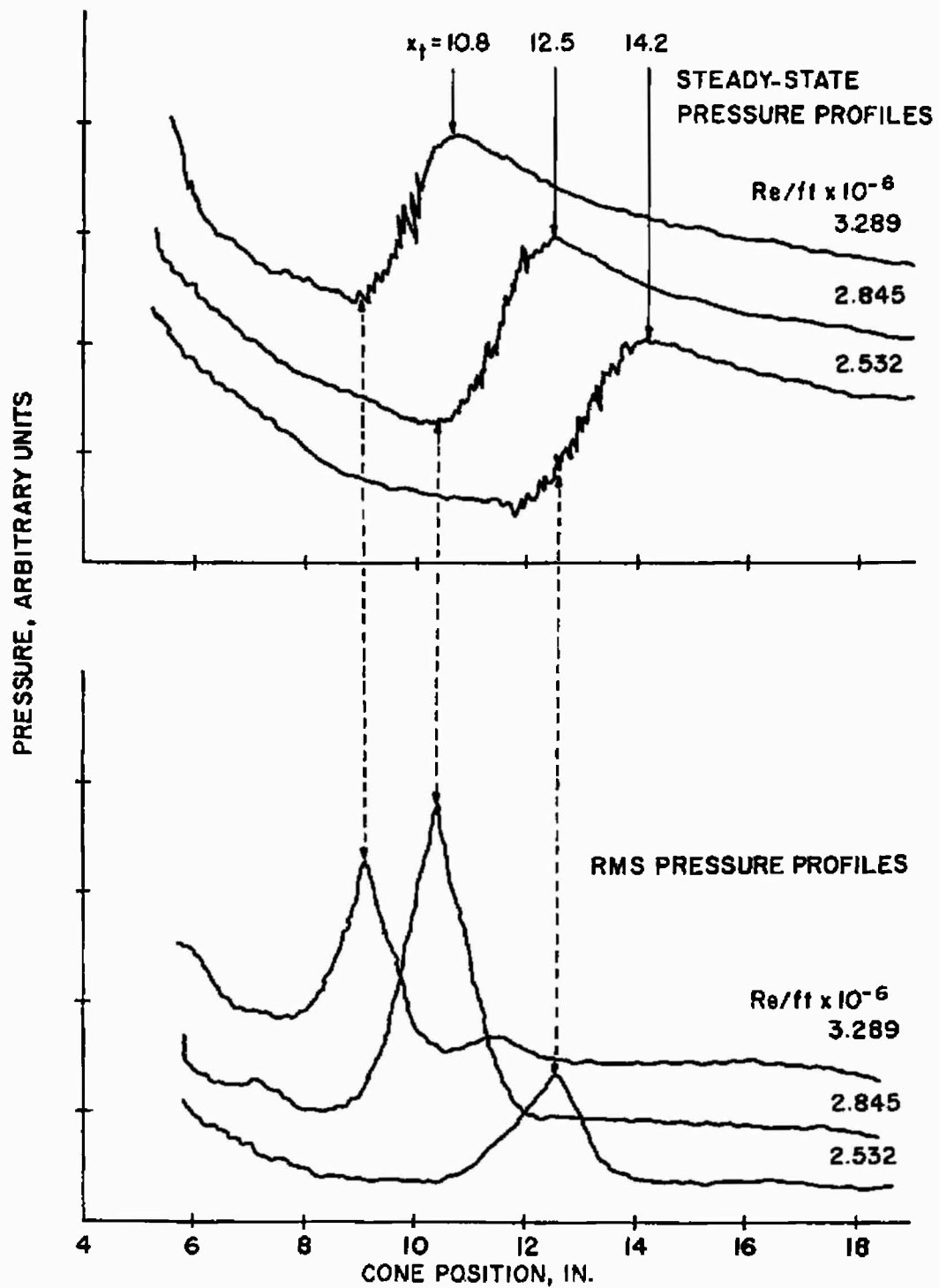
b. $M_\infty = 1.05$
Fig. 10 Concluded

a. $M_\infty = 0.60$ to 0.95
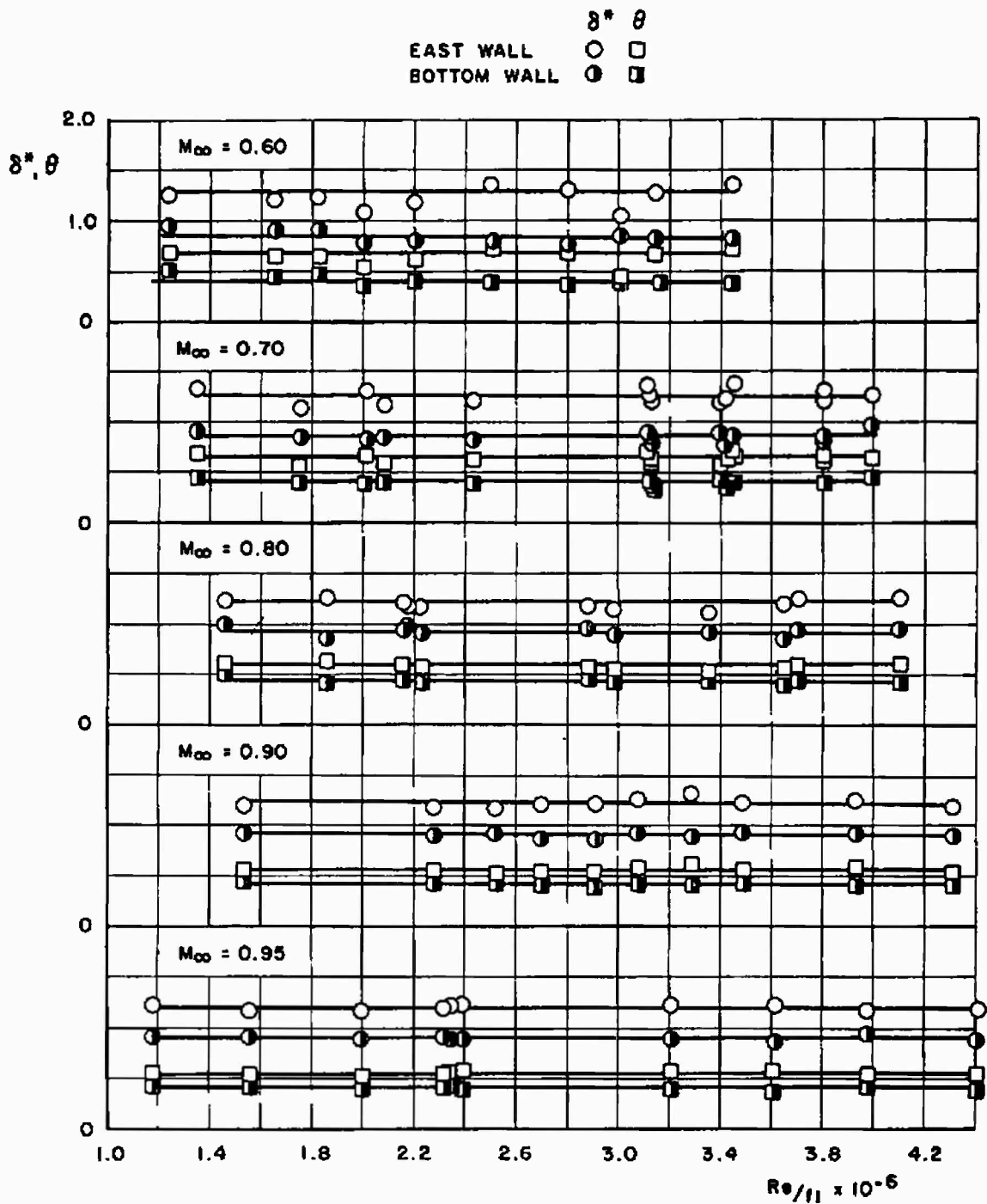
Fig. 11 Variation of Boundary-Layer Displacement and Momentum Thickness with Unit Reynolds Number in Tunnel 16T, Station 12, $\theta_w = 0$ deg
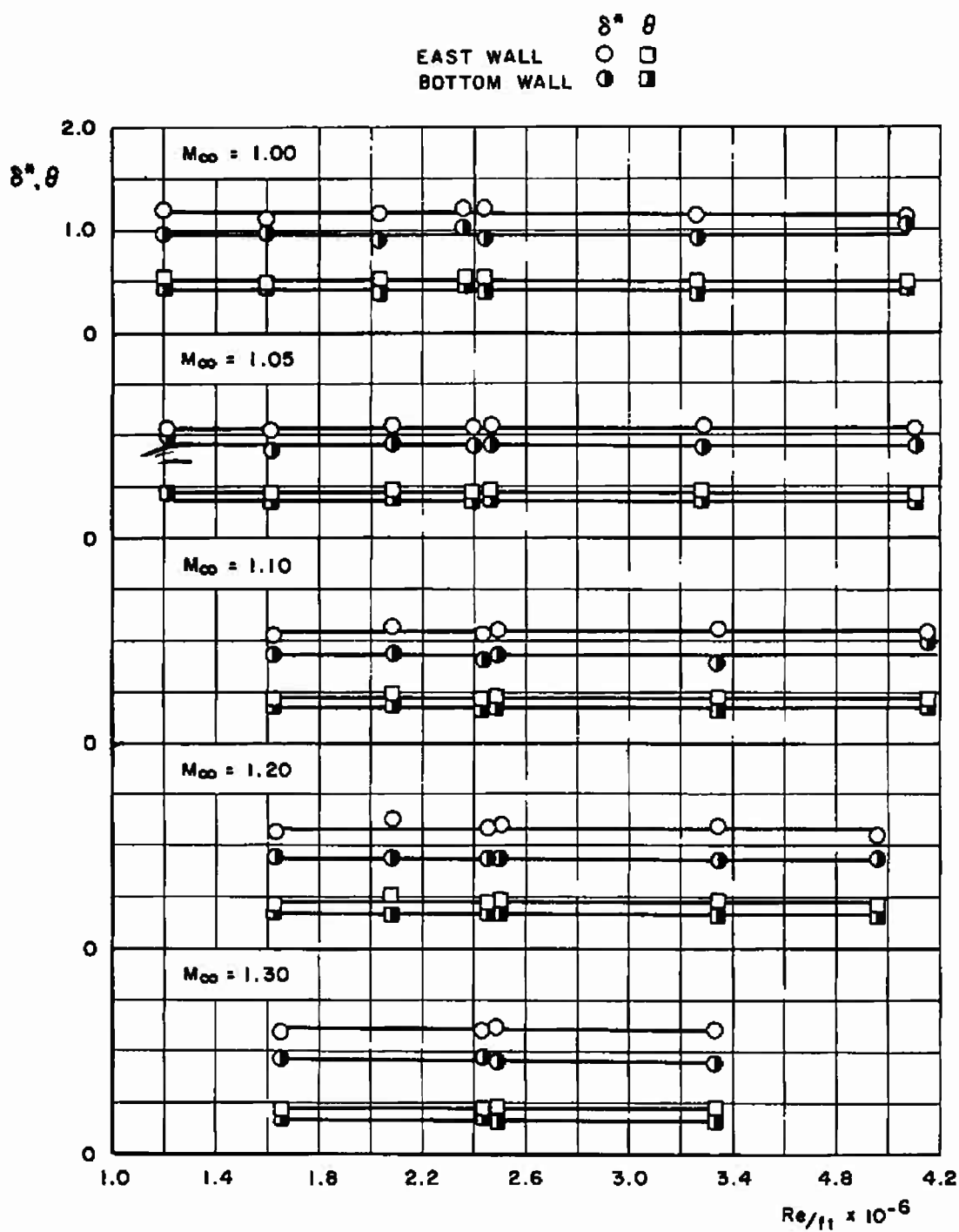
b. M_∞ = 1.00 to 1.30
Fig. 11 Concluded
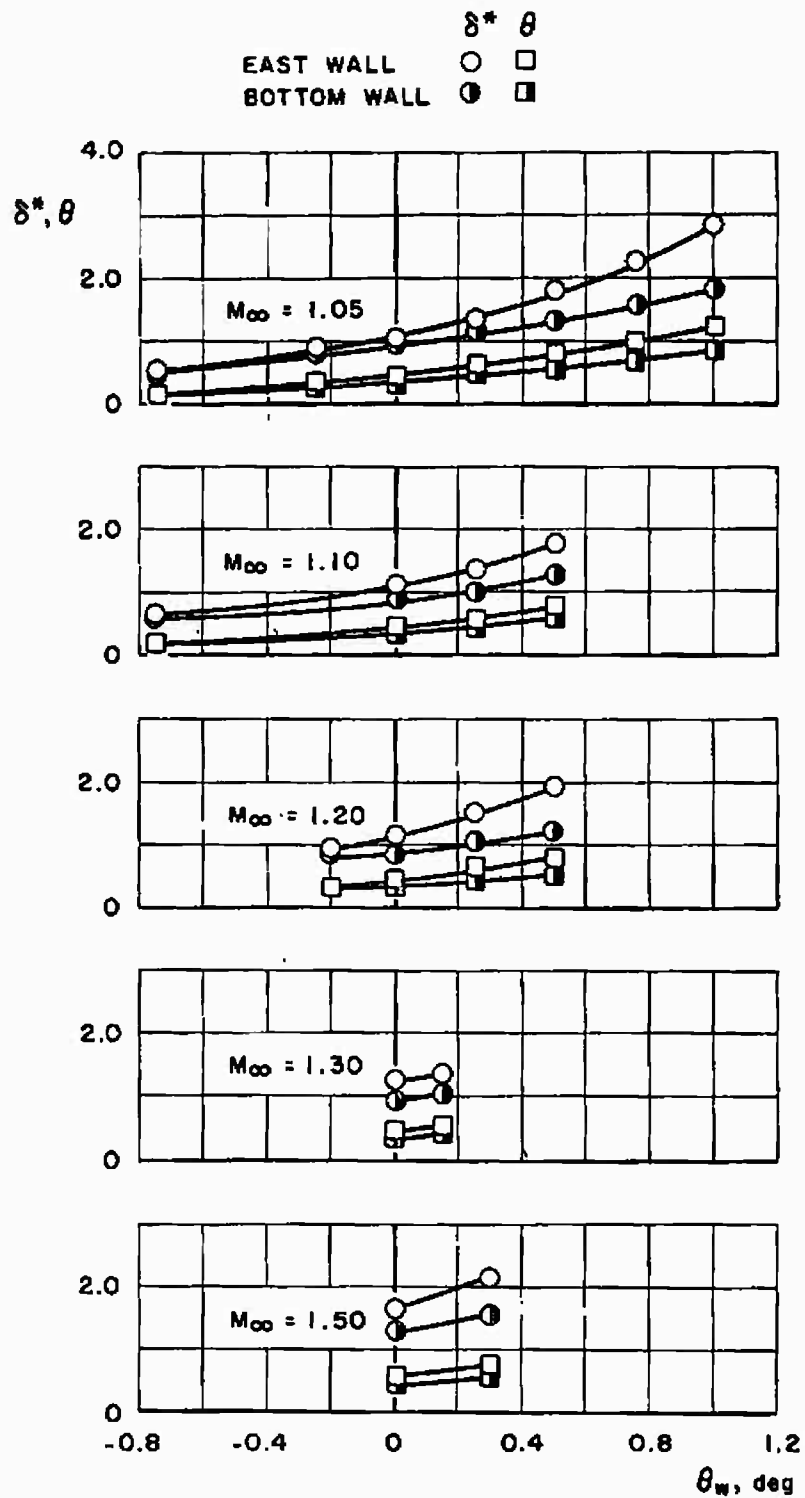
Fig. 12 Variation of Boundary-Layer Displacement and Momentum Thickness with Test Section Wall Angle in Tunnel 16T, Station 12, p_{t_∞} = 800 psfa
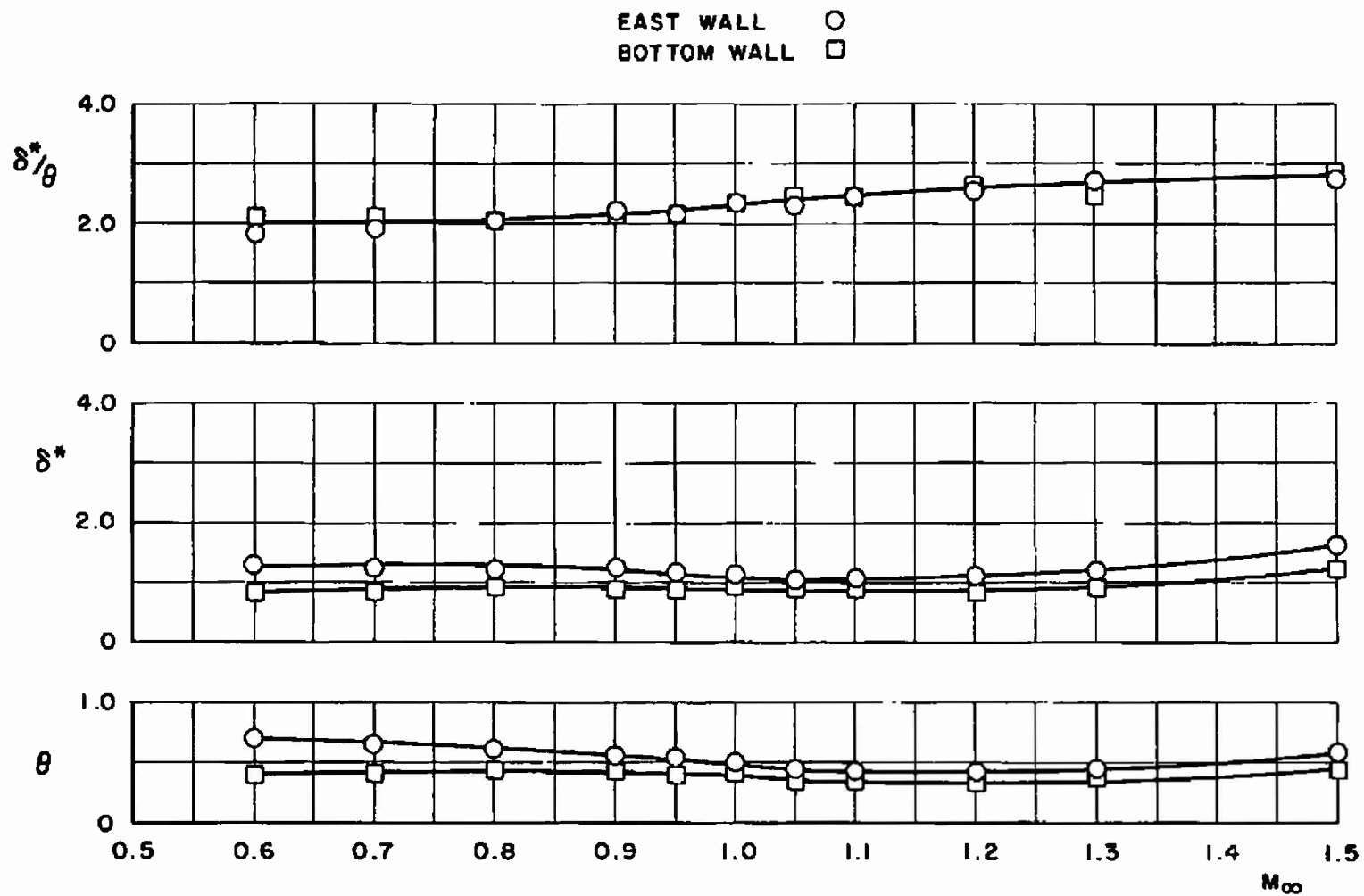
Fig. 13 Variation of Boundary-Layer Shape Factor, Displacement, and Momentum
Thickness with Mach Number in Tunnel 16T, Station 12, p_{t_∞} = 800 psfa,
θ_w = 0 deg
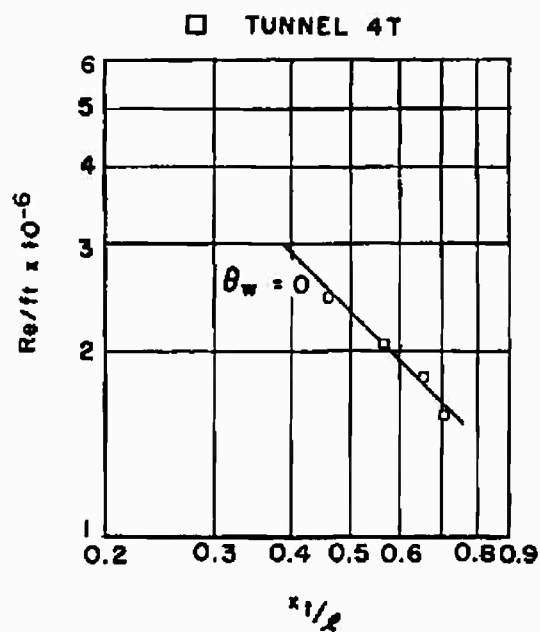
a. $M_\infty = 0.40$
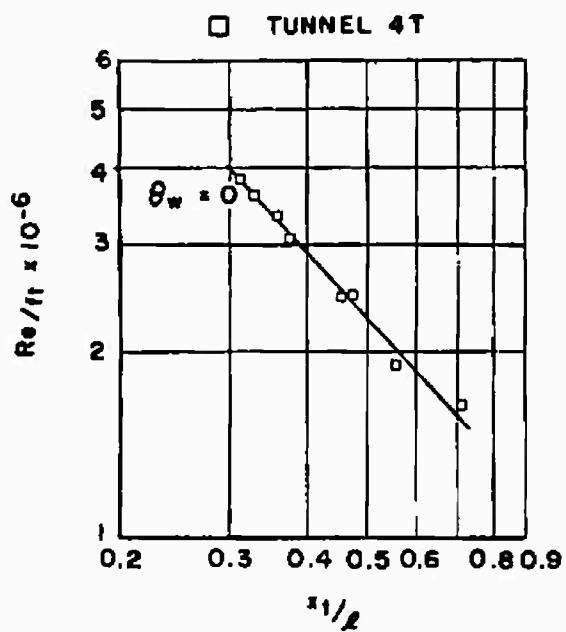
b. $M_\infty = 0.50$
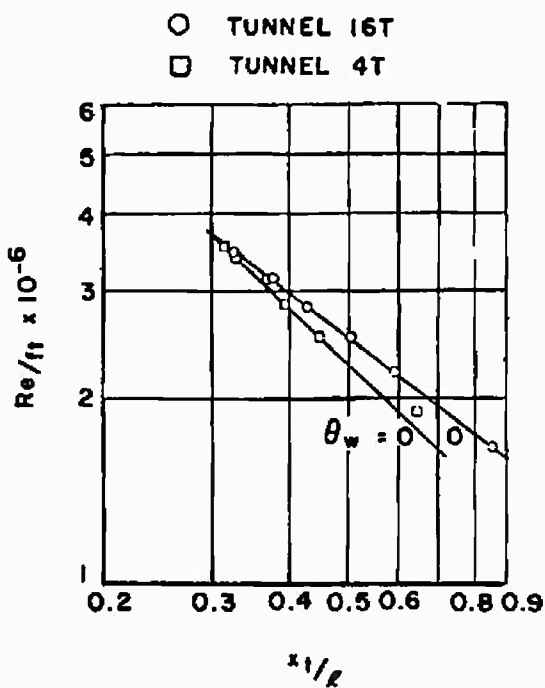
c. $M_\infty = 0.60$
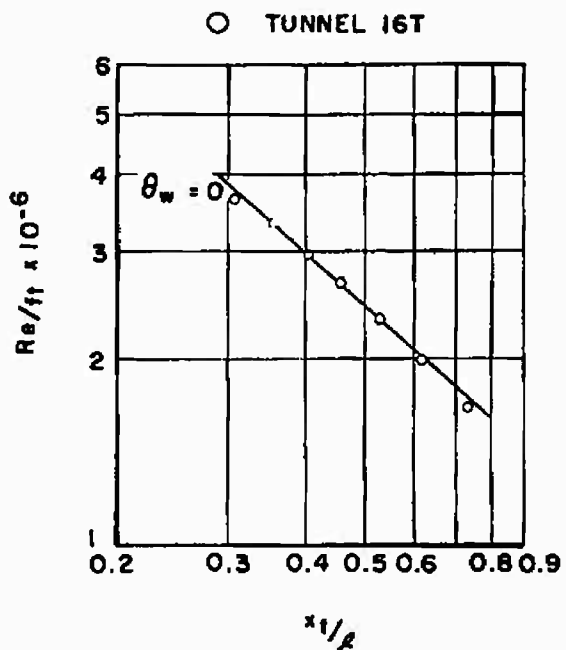
d. $M_\infty = 0.65$

Fig. 14 Variation of Unit Reynolds Number with Nondimensionalized Transition Location for Tunnels 16T and 4T, $\tau = 6.0$ percent

e. $M_\infty = 0.70$

f. $M_\infty = 0.75$

g. $M_\infty = 0.80$

h. $M_\infty = 0.85$

Fig. 14 Continued

i. $M_\infty = 0.90$

j. $M_\infty = 0.95$

k. $M_\infty = 1.00$

l. $M_\infty = 1.05$

Fig. 14 Continued

m. $M_\infty = 1.10$

n. $M_\infty = 1.20$
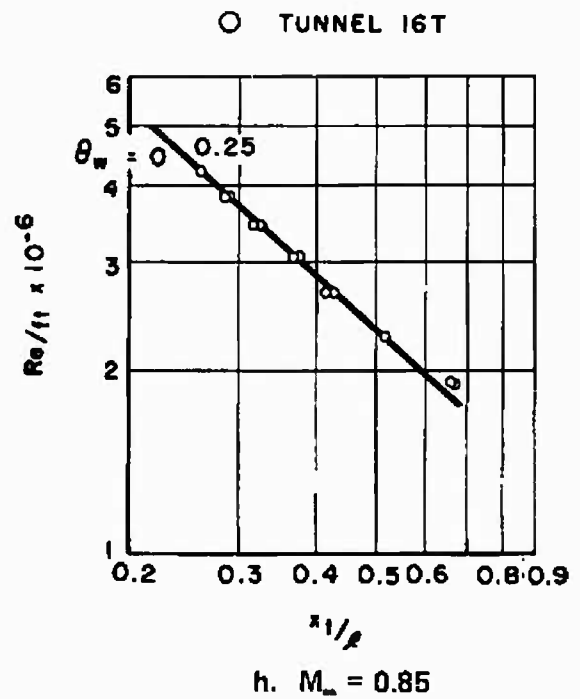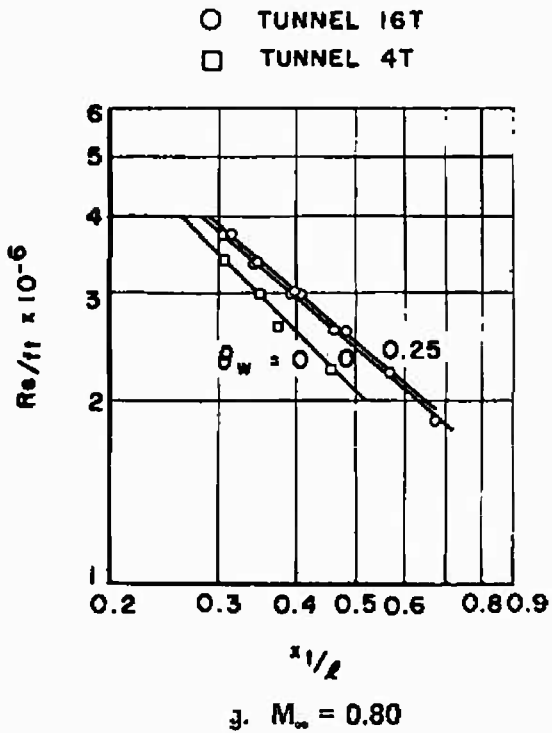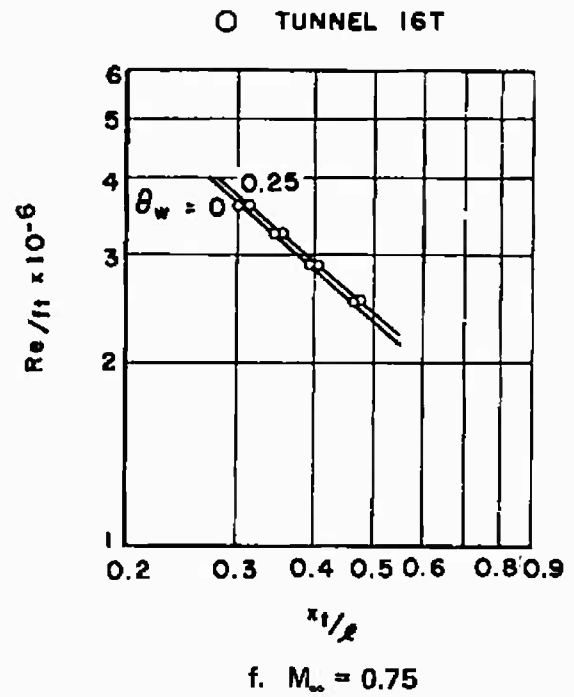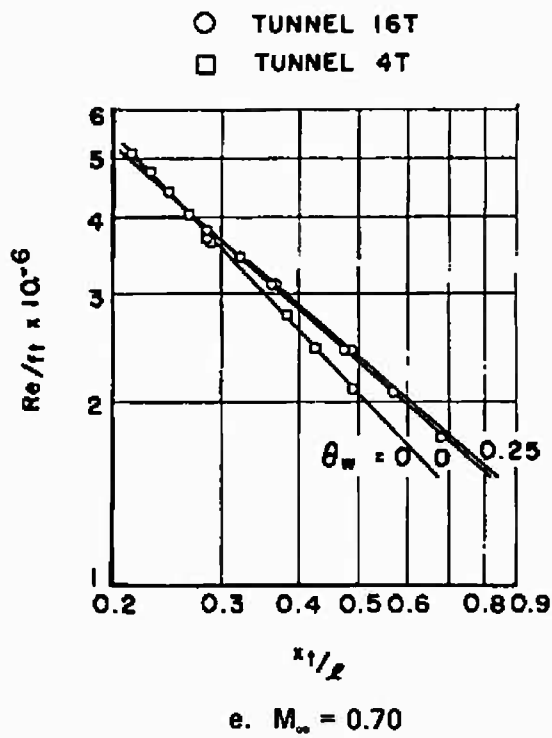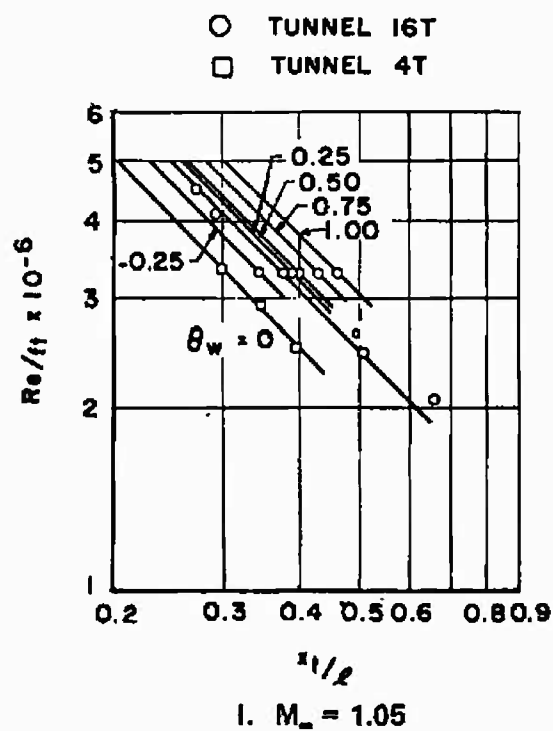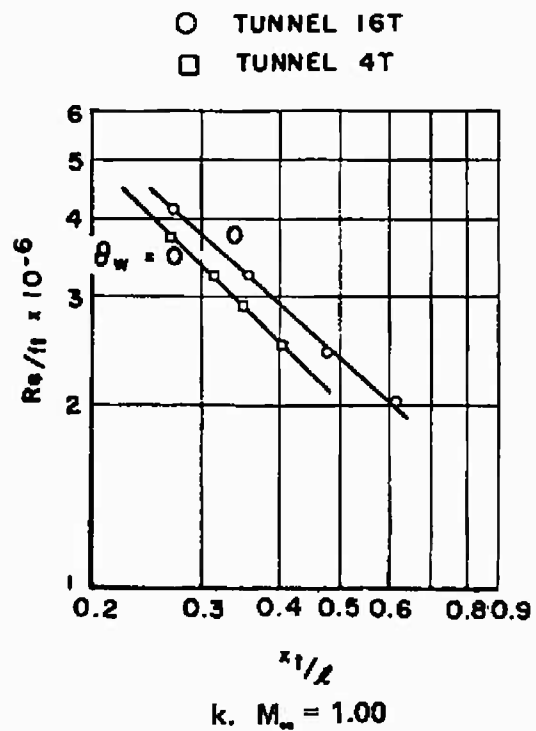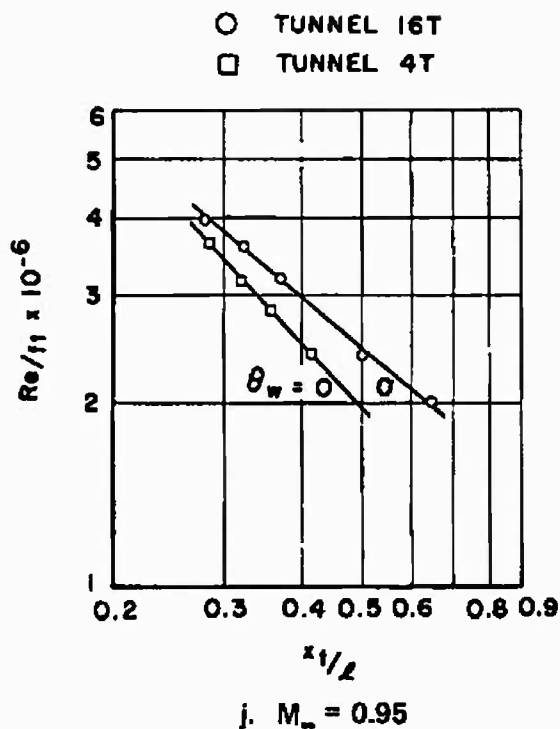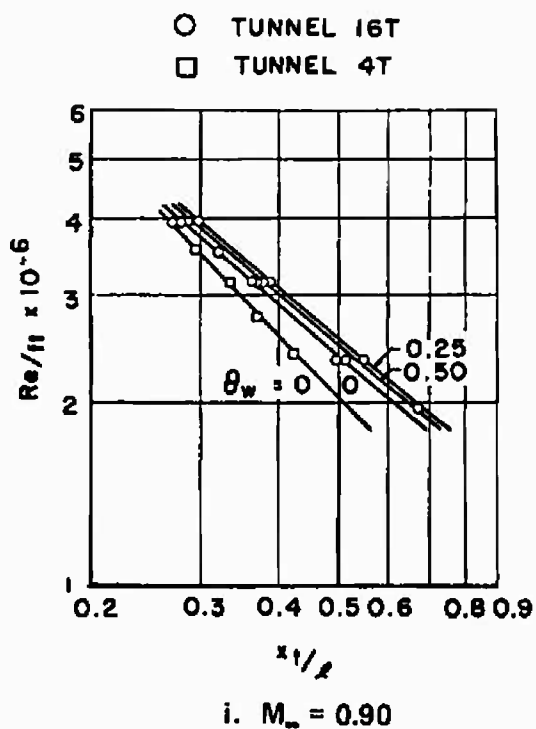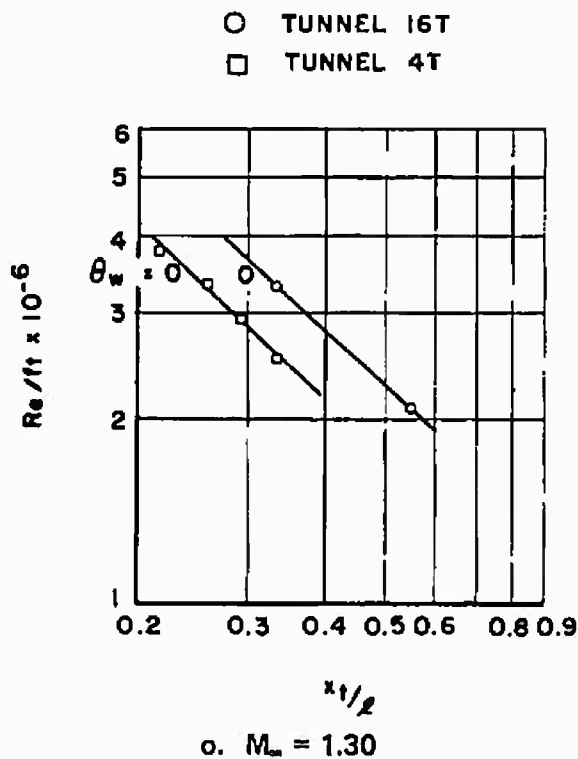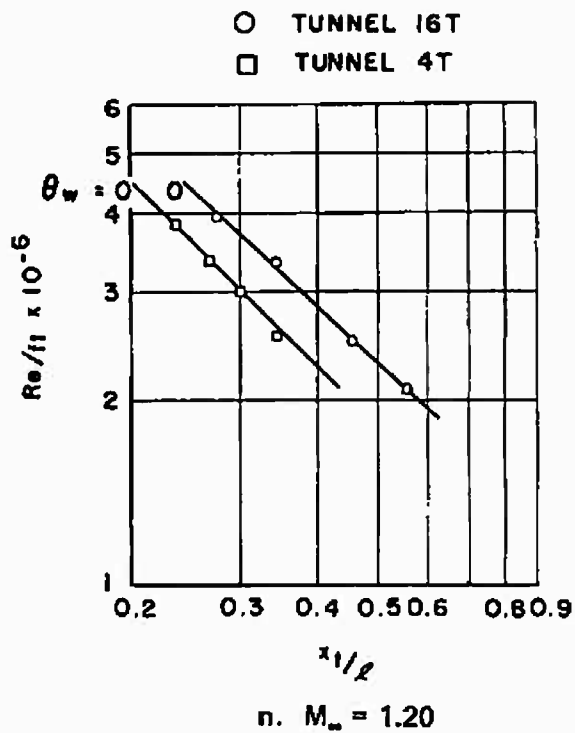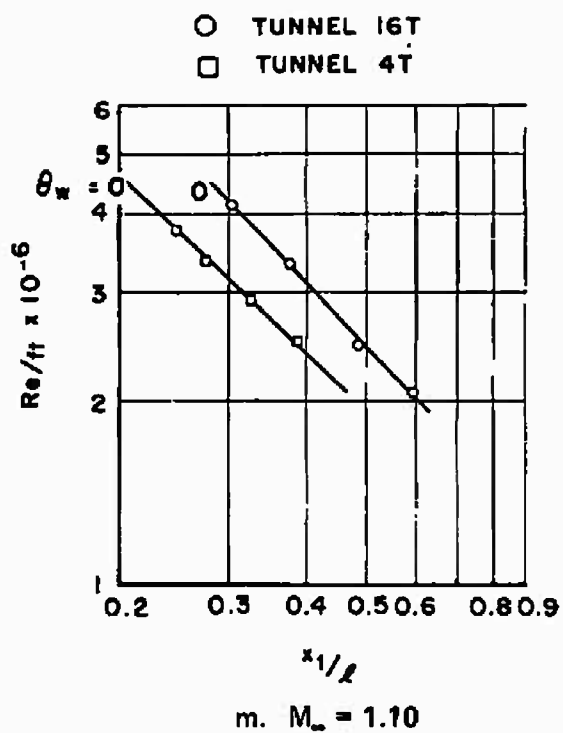
o. $M_\infty = 1.30$
Fig. 14 Concluded
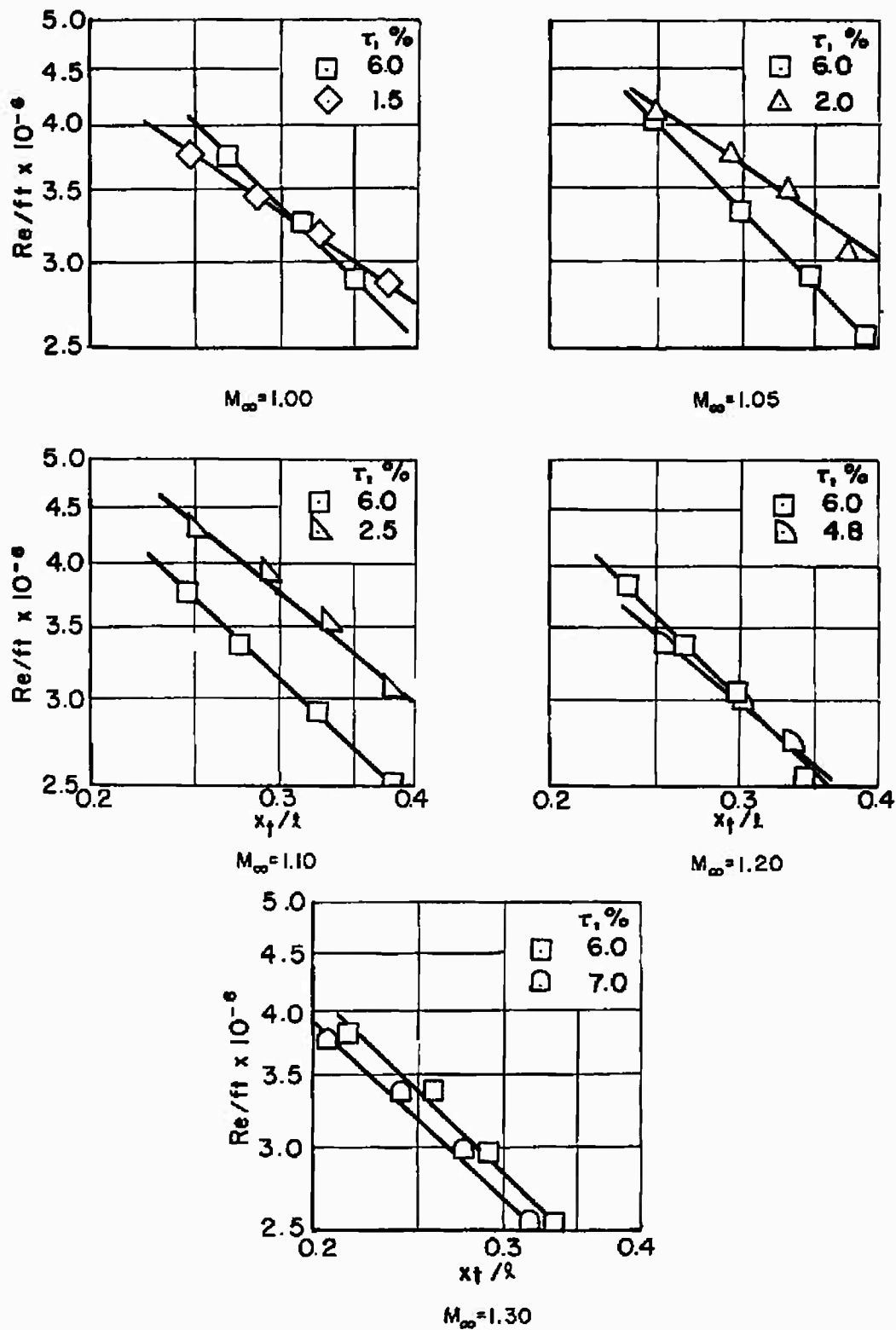
Fig. 15 Variation of Unit Reynolds Number with Nondimensionalized Transition
Location for Selected Wall Porosities in Tunnel 4T
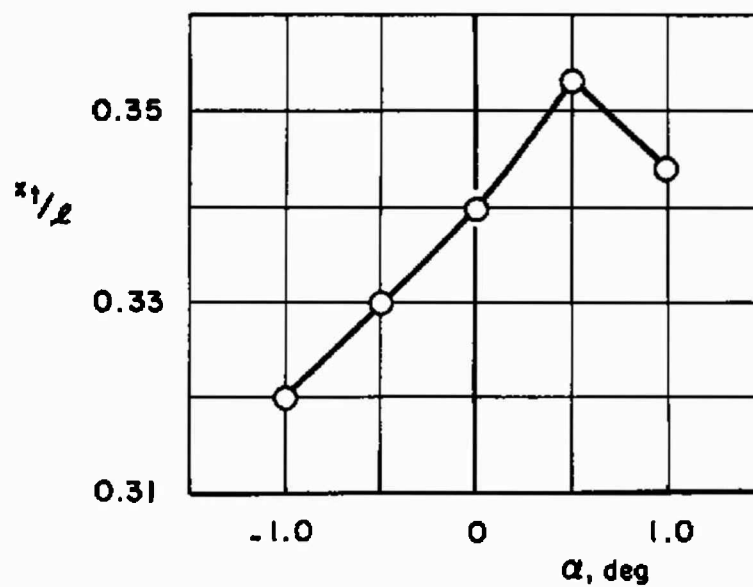
Fig. 16 Variation of Nondimensionalized Transition Location with Cone Angle of Attack in Tunnel 16T, $M_\infty = 0.80$, Re/ft = 3.35 x 10^6
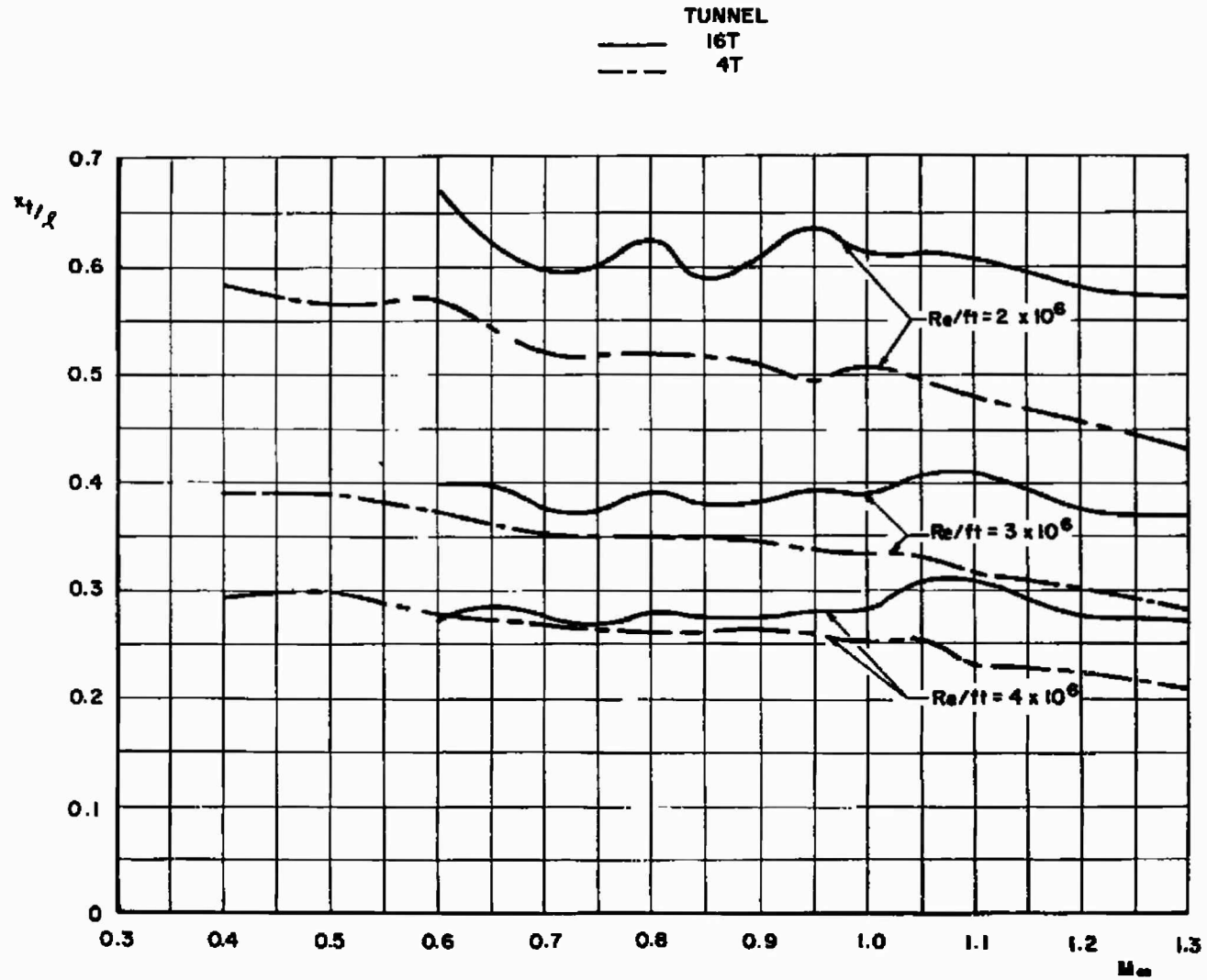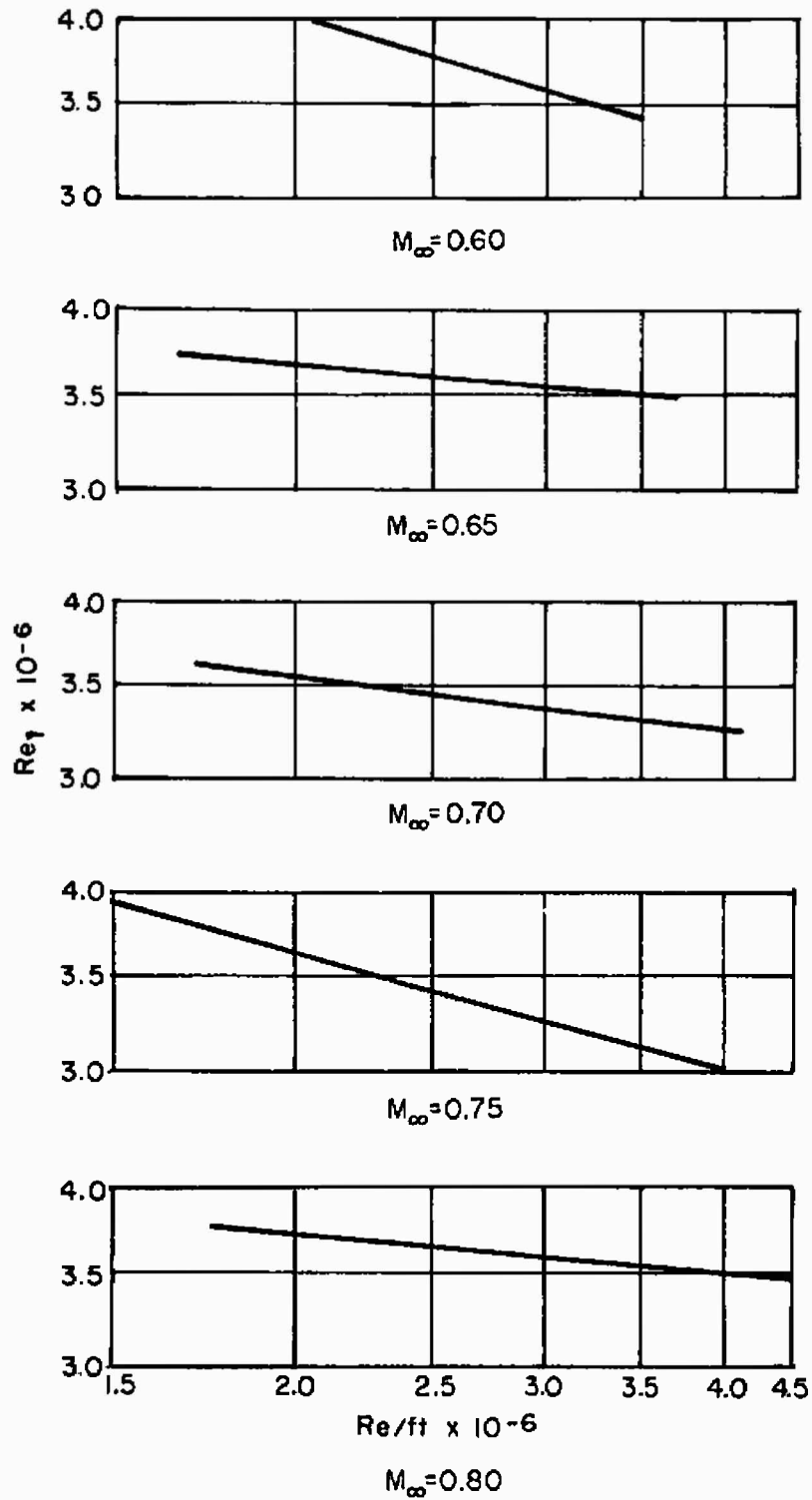
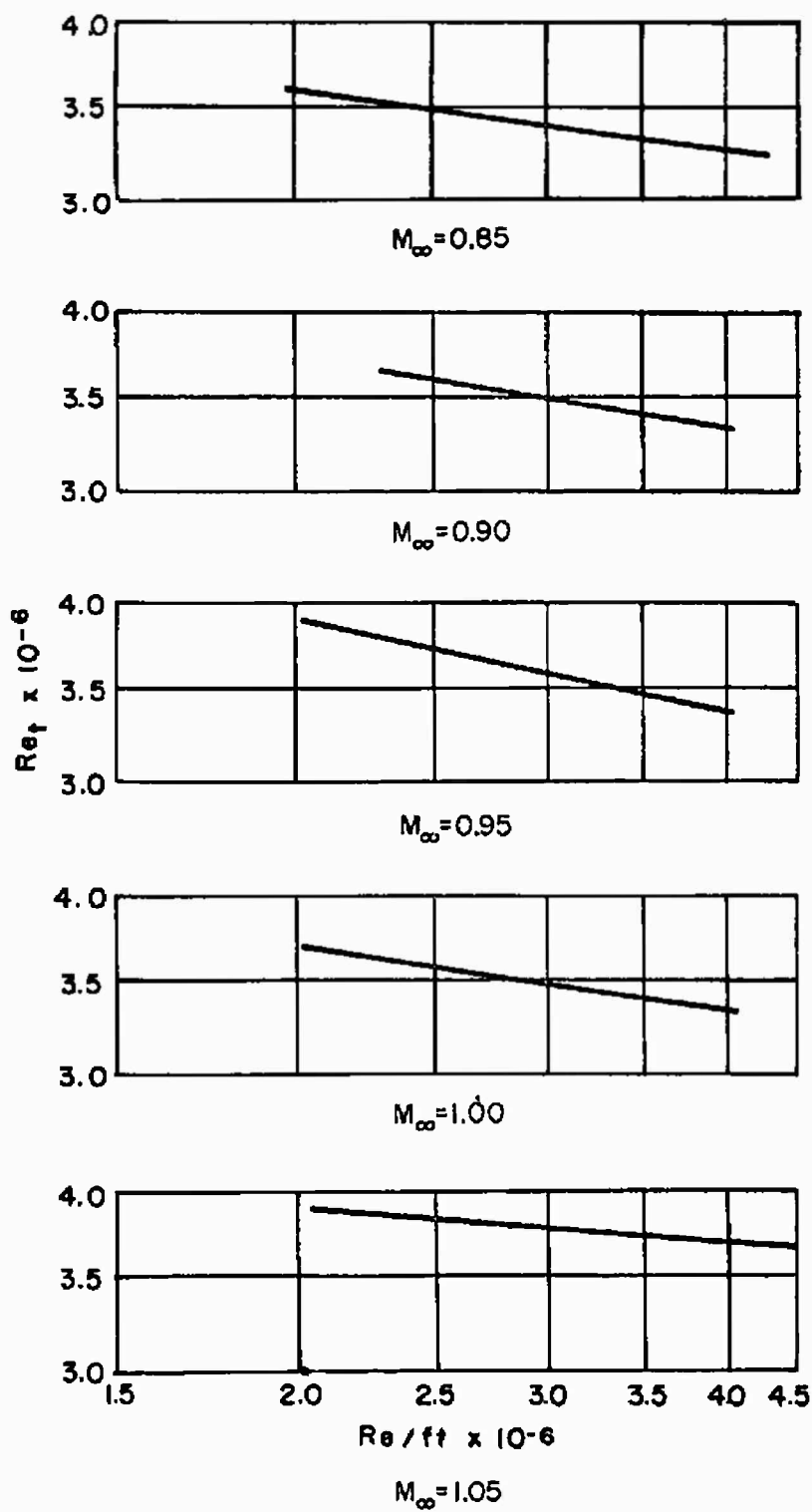Fig. 17 Variation of Nondimensionalized Transition Location with Mach
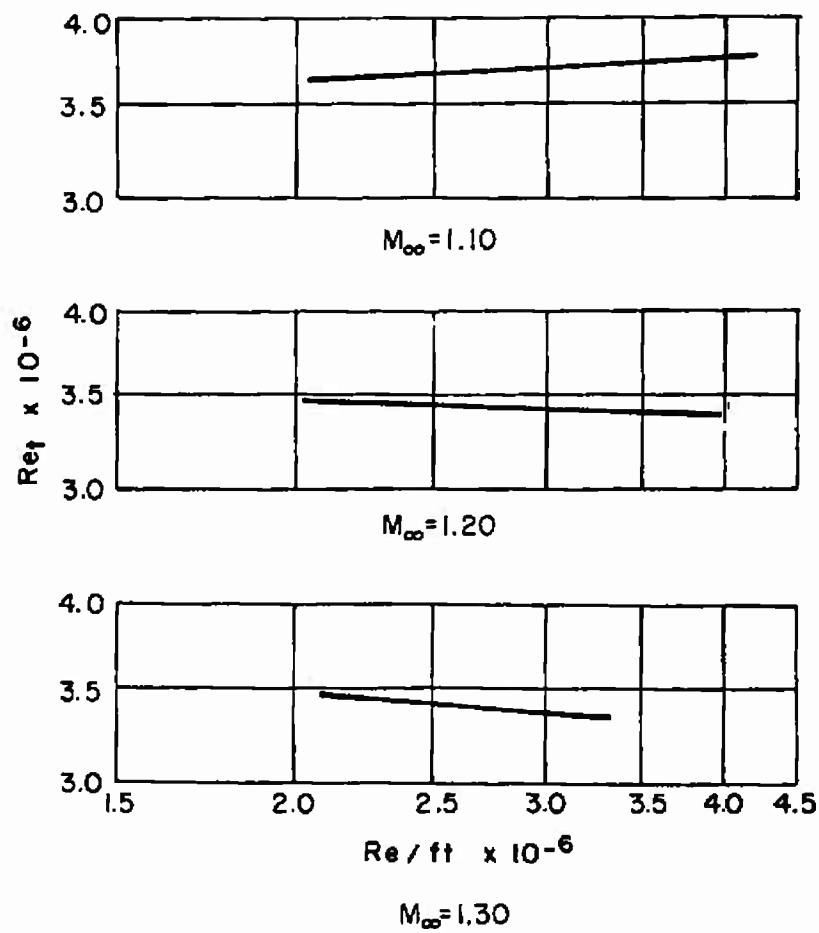Number for Constant Unit Reynolds Number, $\theta_w = 0$ deg

a. $M_\infty = 0.60$ to 0.80

Fig. 18 Variation of Transition Reynolds Number with Unit Reynolds Number for Tunnel 16T, $\theta_w = 0$ deg
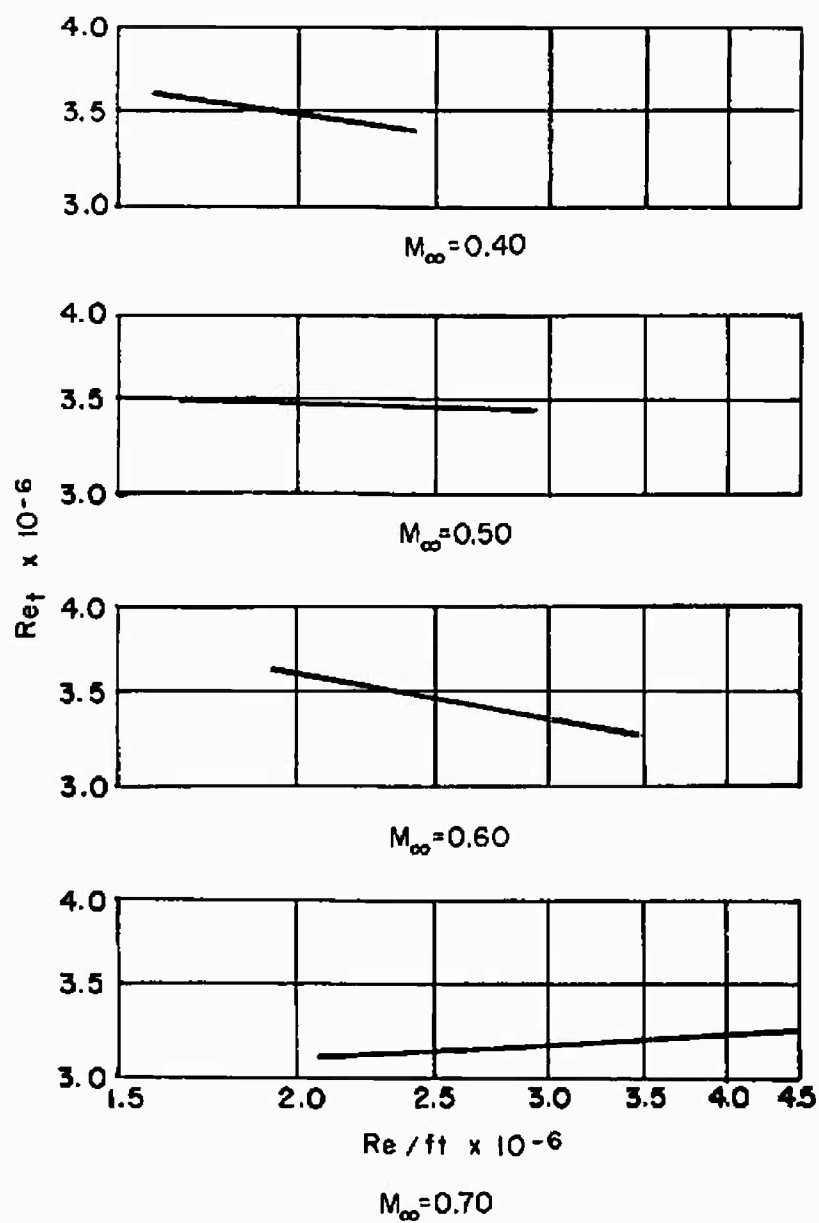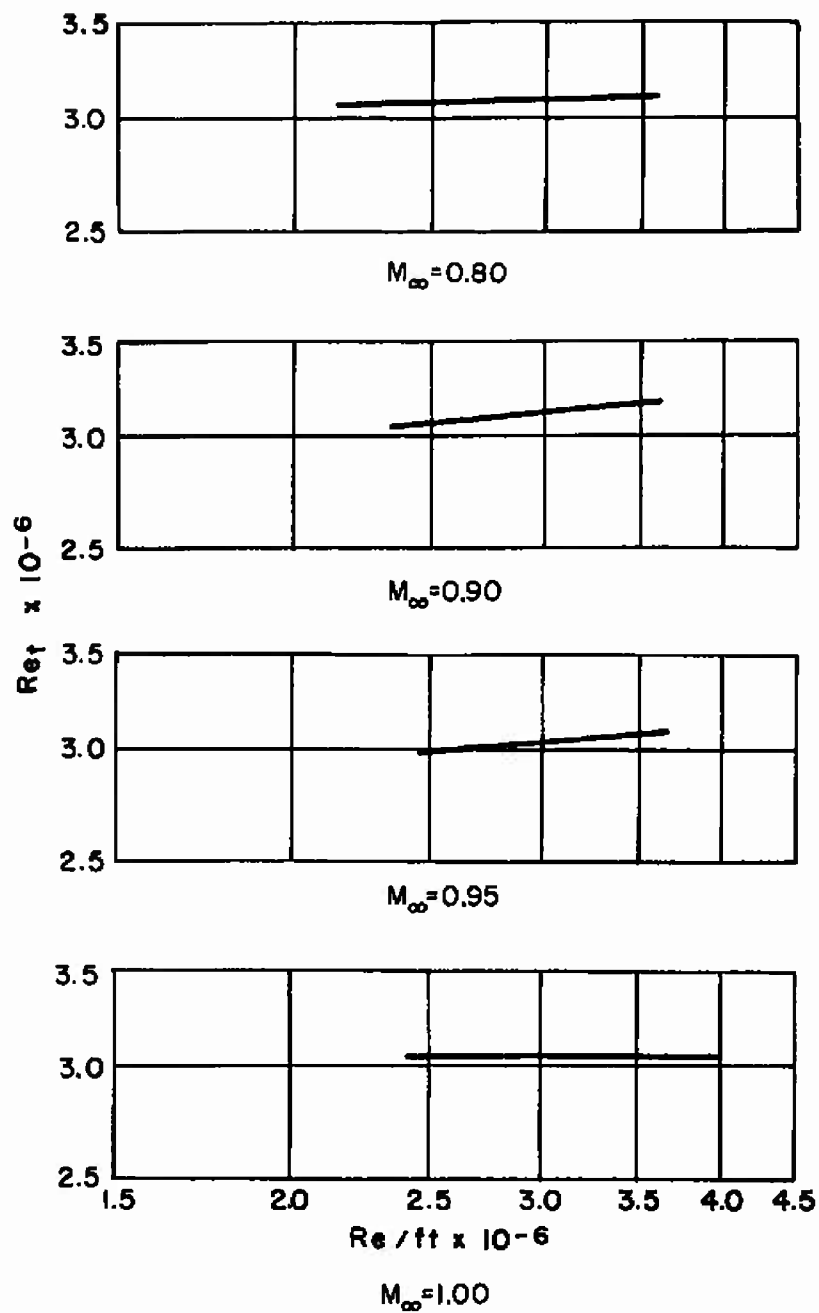
b. M_∞ = 0.85 to 1.05
Fig. 18 Continued

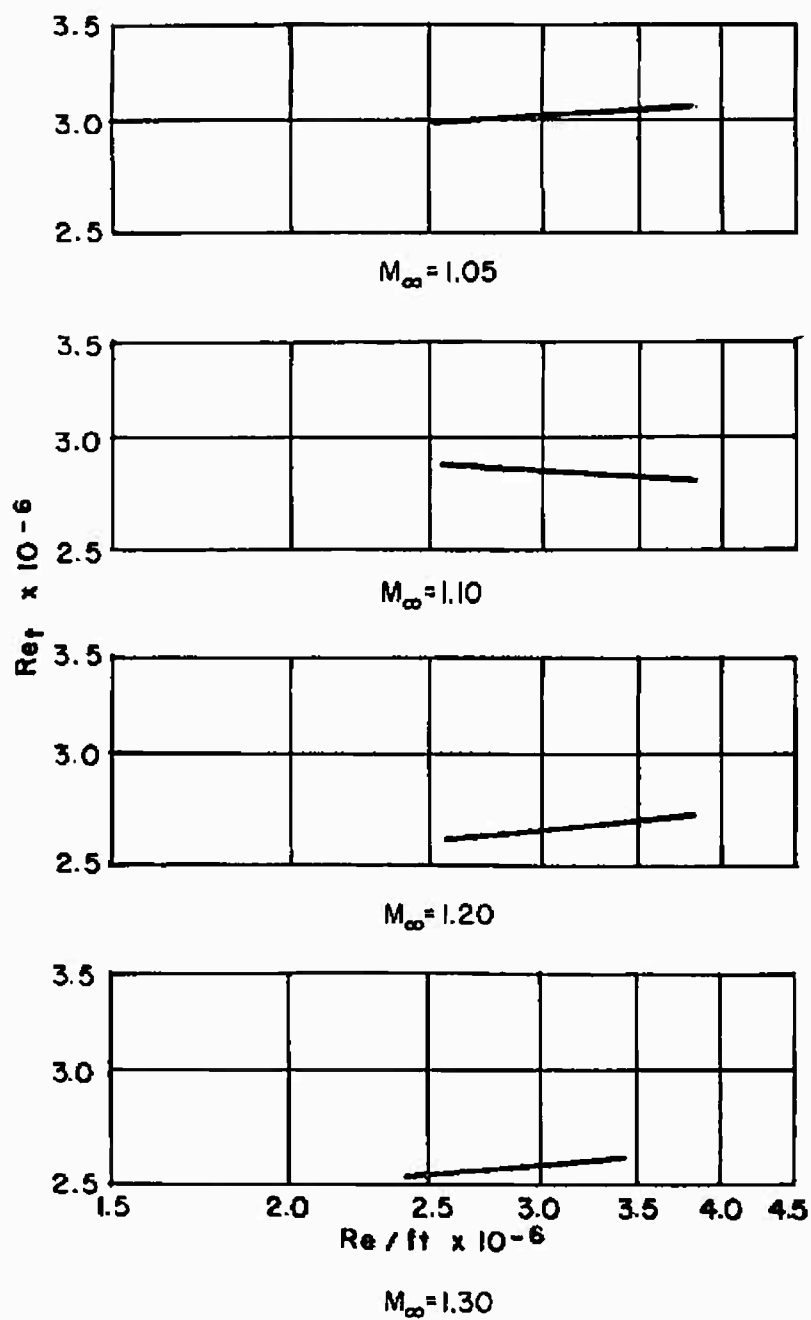c. $M_\infty = 1.10$ to 1.30
Fig. 18 Concluded

a. M_∞ = 0.40 to 0.70
Fig. 19 Variation of Transition Reynolds Number with Unit Reynolds Number for Tunnel 4T, r = 6.0 percent, θ_w = 0 deg

b. $M_\infty = 0.80$ to 1.00
Fig. 19 Continued

c. M_∞ = 1.05 to 1.30
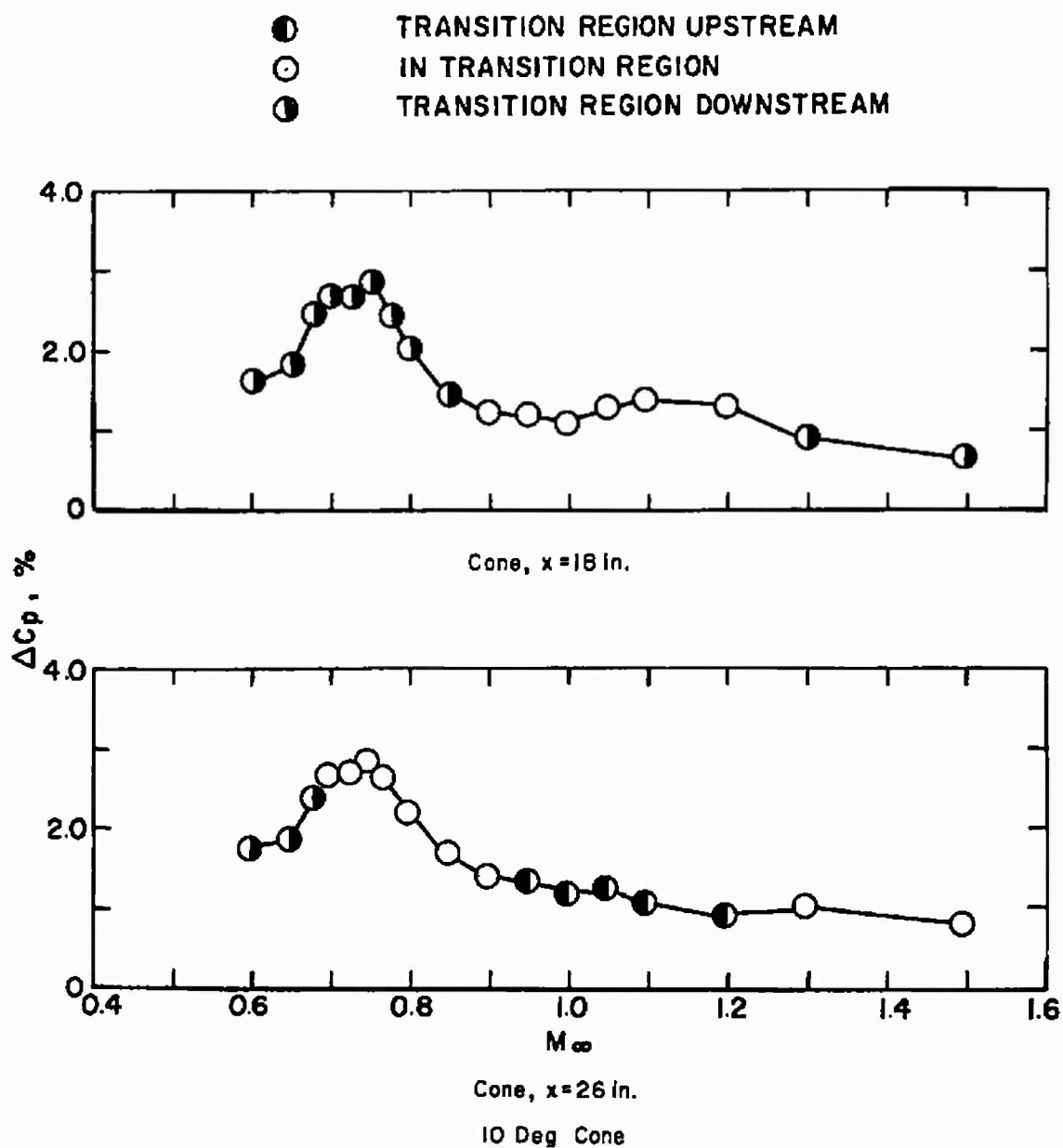Fig. 19 Concluded

Fig. 20 Evaluation of the Overall rms Noise Levels in Tunnel 16T
with Respect to Transition Location, p_{t_∞} = 800 psfa

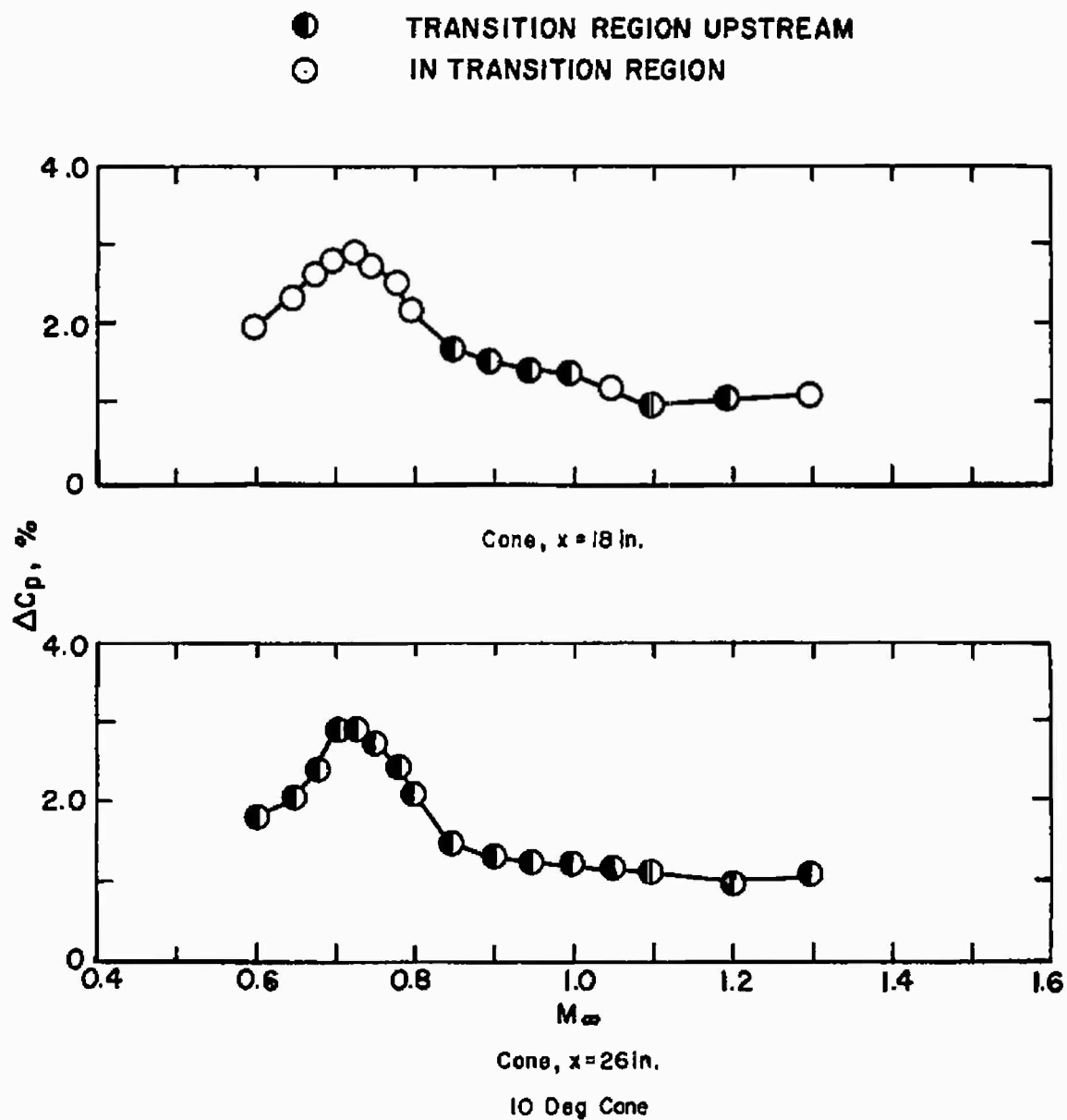Fig. 21 Evaluation of the Overall rms Noise Levels in Tunnel 16T with Respect to Transition Location, $p_{t_\infty} = 1185$ psfa
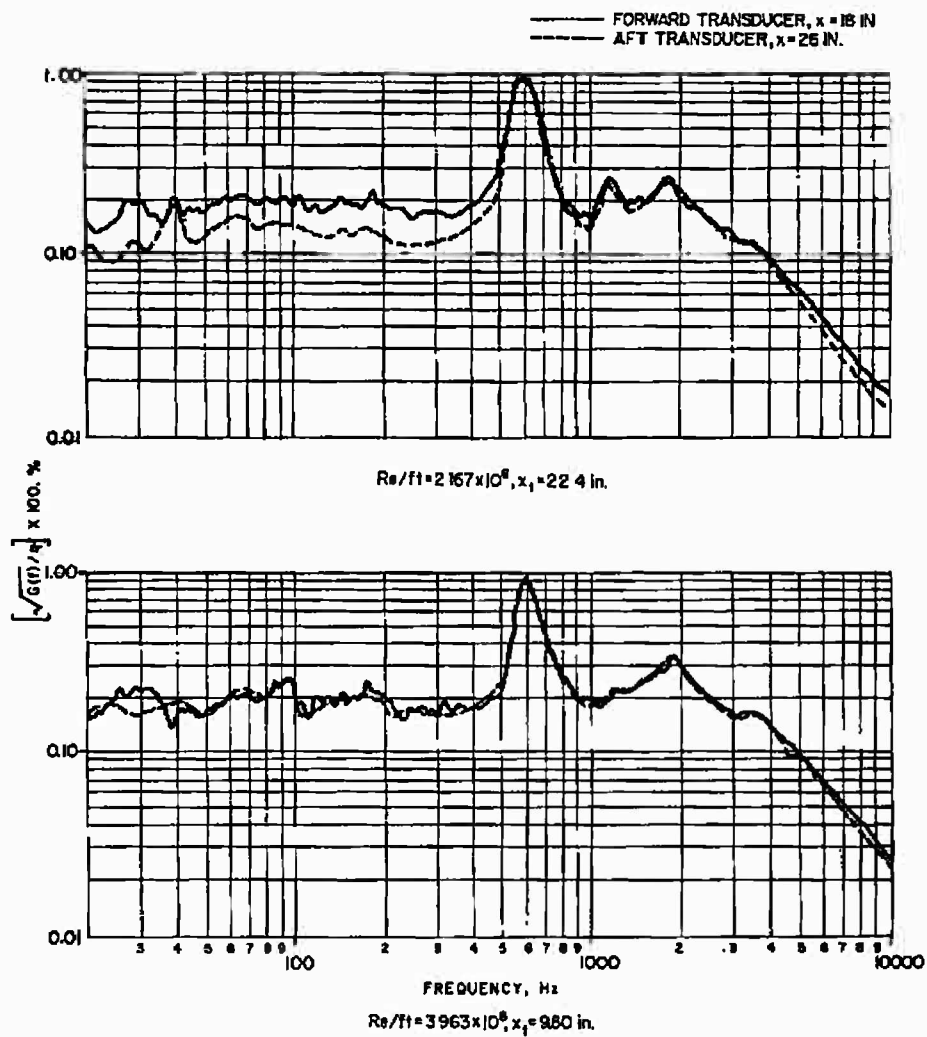
Fig. 22 Comparison of Frequency Spectra Relative to Transition Location on the 10-deg Cone in Tunnel 16T, $M_\infty = 0.75$

Fig. 23 Comparison of Frequency Spectra Relative to Transition Location
on the 10-deg Cone in Tunnel 16T, $M_\infty = 1.10$

TUNNEL

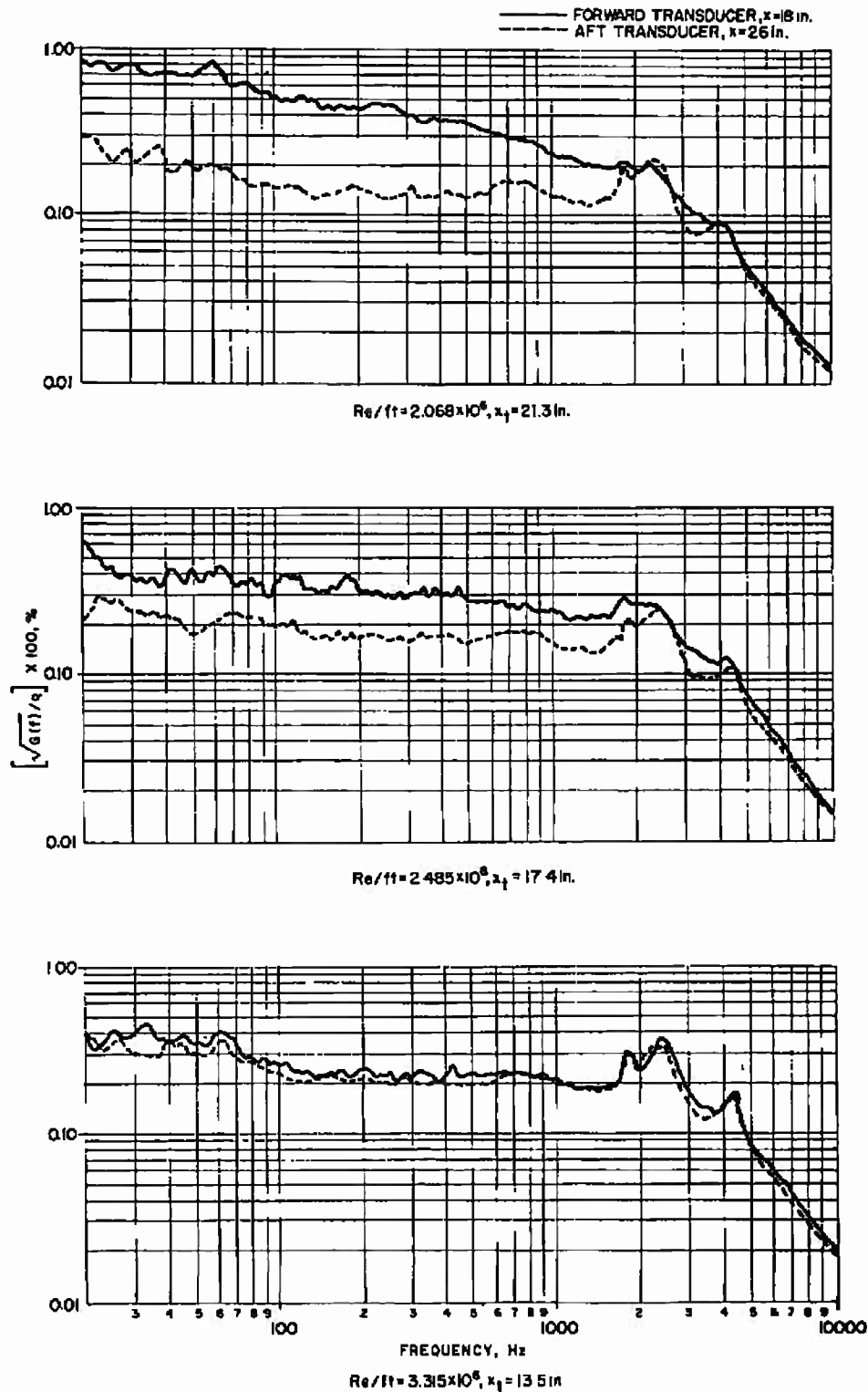16T   4T

◐   ◧   TRANSITION REGION UPSTREAM

       □   IN TRANSITION REGION
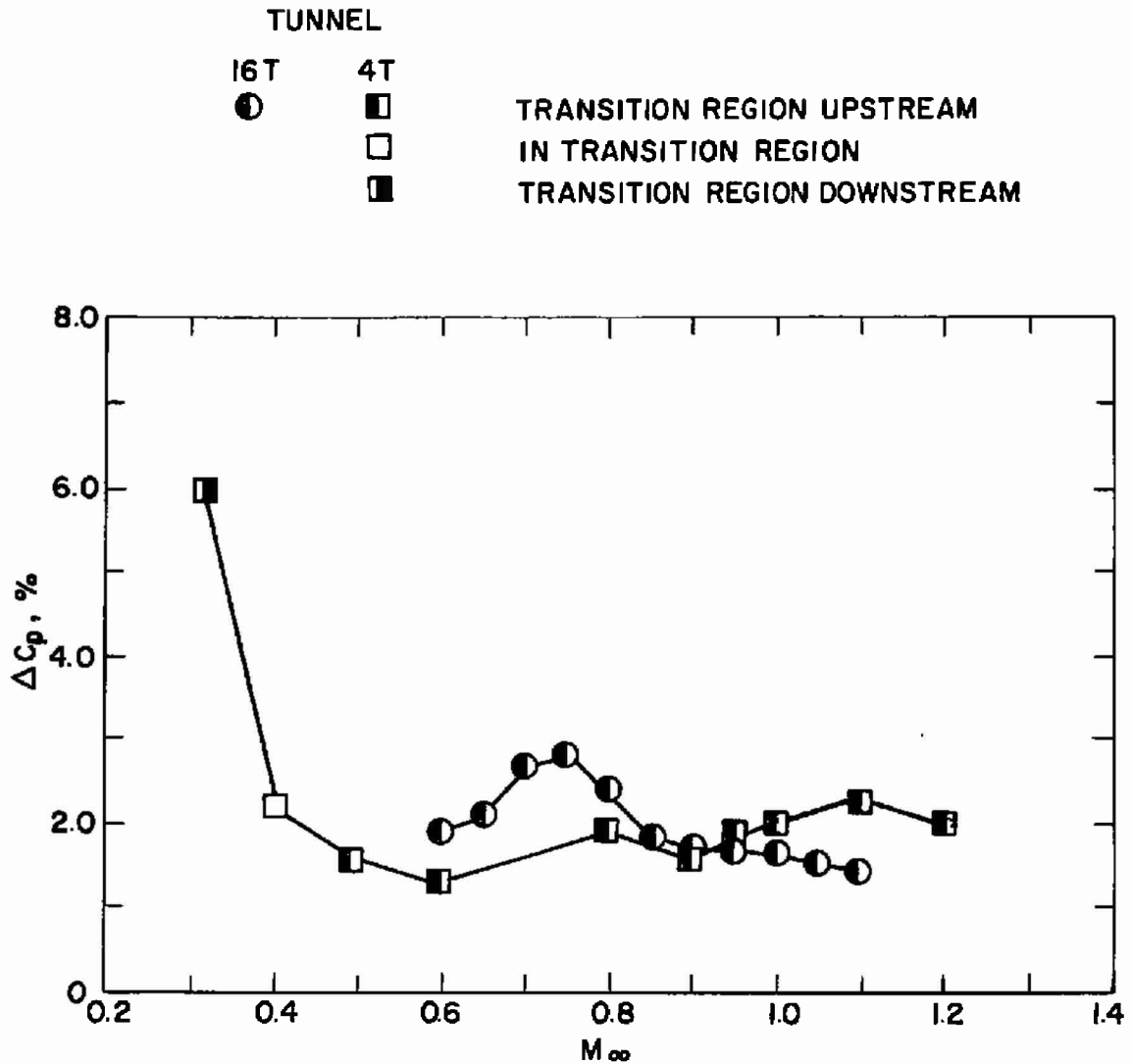
       ◨   TRANSITION REGION DOWNSTREAM

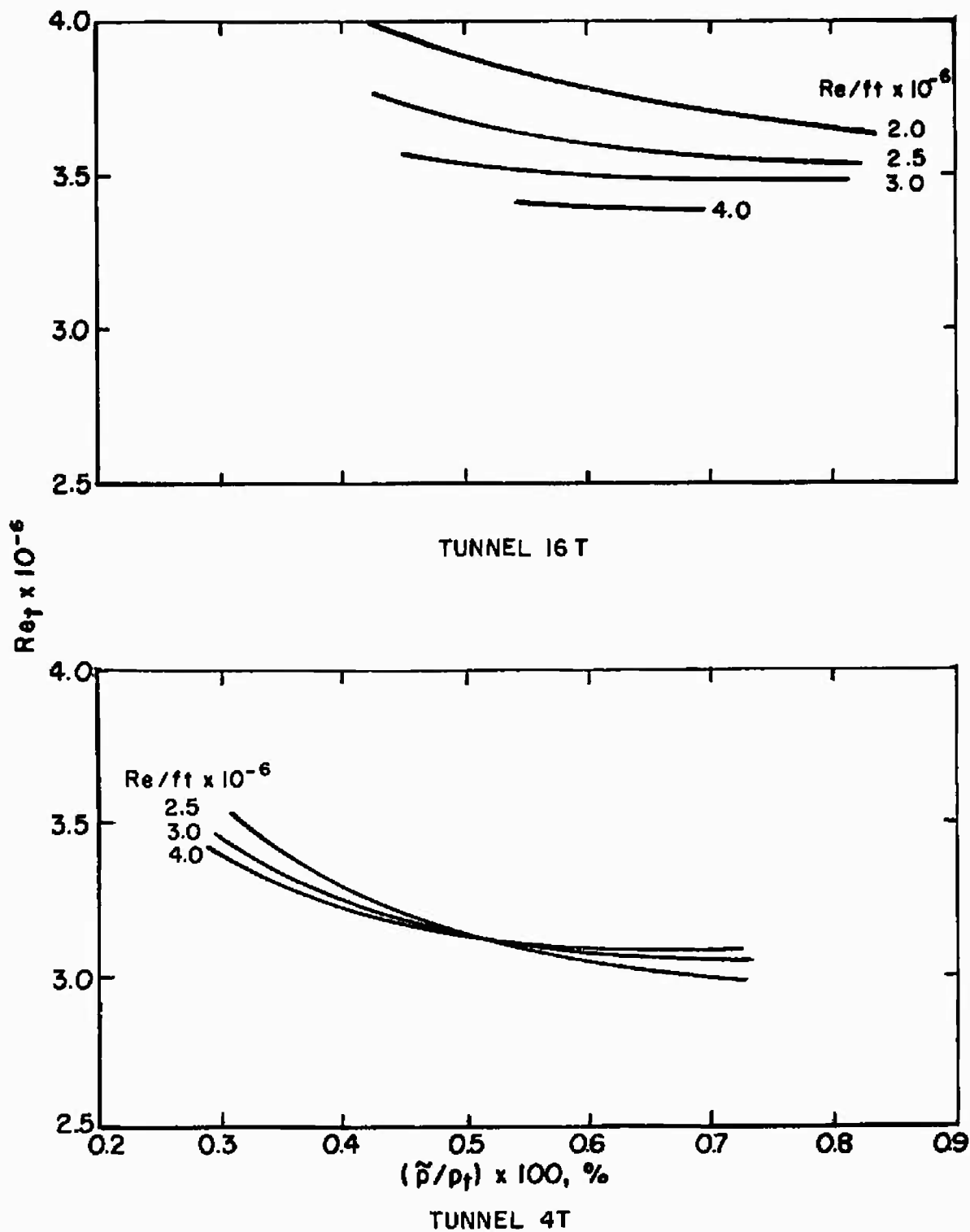Fig. 24 Comparison of Noise Levels in Tunnels 16T and 4T, p_{t_∞} = 1800 psfa

Fig. 25 Correlation of Transition Reynolds Number and Test Section Noise
Levels in Tunnels 16T and 4T, τ = 6.0 percent, $0.60 \leqslant M_\infty \leqslant 1.00$

DOCUMENT CONTROL DATA - R & D

(Security classification of title, body of abstract and indexing annotation must be entered when the overall report is classified)

1. ORIGINATING ACTIVITY *(Corporate author)*	2a. REPORT SECURITY CLASSIFICATION
Arnold Engineering Development Center ARO, Inc., Operating Contractor Arnold Air Force Station, Tennessee 37389	UNCLASSIFIED
	2b. GROUP N/A

3. REPORT TITLE

DETERMINATION OF TRANSITION REYNOLDS NUMBER IN THE TRANSONIC MACH NUMBER RANGE

4. DESCRIPTIVE NOTES *(Type of report and inclusive dates)*

Final Report December 1969 to June 1970

5. AUTHOR(S) *(First name, middle initial, last name)*

O. P. Credle and W. E. Carleton, ARO, Inc.

6. REPORT DATE	7a. TOTAL NO. OF PAGES	7b. NO. OF REFS
October 1970	57	6

8a. CONTRACT OR GRANT NO.	9a. ORIGINATOR'S REPORT NUMBER(S)
F40600-71-C-0002	
b. PROJECT NO.	AEDC-TR-70-218
c. Program Element 65401F/G226	9b. OTHER REPORT NO(S) *(Any other numbers that may be assigned this report)*
d.	ARO-PWT-TR-70-242

10. DISTRIBUTION STATEMENT This document is subject to special export controls and each transmittal to foreign governments or foreign nationals may be made only with prior approval of Arnold Engineering Development Center (XON), Arnold Air Force Station, Tennessee 37389.

11. SUPPLEMENTARY NOTES	12. SPONSORING MILITARY ACTIVITY
Available in DDC	Arnold Engineering Development Center, XON, Arnold Air Force Station, Tennessee 37389.

13. ABSTRACT

This report presents the results of an investigation to determine the transition Reynolds number characteristics of the Propulsion Wind Tunnel (16T) and the Aerodynamic Wind Tunnel (4T) by measuring the location of boundary-layer transition on a 10-deg total-angle cone. Boundary-layer thickness on the test section walls and test section noise levels were measured in an attempt to determine their influence on boundary-layer transition location. Transition Reynolds number decreased with increasing Mach number in both tunnels with a higher rate of change in Tunnel 4T. Transition Reynolds number decreased with increasing unit Reynolds number for free-stream Mach numbers < 1.0 and alternated between decreasing and increasing with increasing unit Reynolds number for free-stream Mach numbers > 1.0. Test results indicated that boundary-layer transition on the cone surface was affected by test section wall angle, wall porosity, and the noise radiating from the test section walls. The boundary-layer acoustic level, as measured on the cone surface, was relatively unaffected by transition location for subsonic Mach numbers.

DD FORM 1473 I NOV 65

14. KEY WORDS	LINK A		LINK B		LINK C	
	ROLE	WT	ROLE	WT	ROLE	WT
conical bodies						
transonic wind tunnels						
Reynolds number						
boundary-layer transition						
acoustics						
noise (sound)						